The Journal of Immunology

RESEARCH ARTICLE | MARCH 01 2022

Exon–Intron Circular RNA circRNF217 Promotes Innate Immunity and Antibacterial Activity in Teleost Fish by Reducing miR-130-3p Function FREE

Weiwei Zheng; ... et. al

J Immunol (2022) 208 (5): 1099–1114.
https://doi.org/10.4049/jimmunol.2100890

Exon–Intron Circular RNA circRNF217 Promotes Innate Immunity and Antibacterial Activity in Teleost Fish by Reducing miR-130-3p Function

Weiwei Zheng,*,[1] Hui Su,*,[1] Xing Lv,* Shiying Xin,* and Tianjun Xu*,†,‡,§

Circular RNA (circRNA) is produced by splicing head to tail and is widely distributed in multicellular organisms, and circRNA reportedly can participate in various cell biological processes. In this study, we discovered a novel exon–intron circRNA derived from probable E3 ubiquitin-protein ligase RNF217 (*RNF217*) gene, namely, circRNF217, which was related to the antibacterial responses in teleost fish. Results indicated that circRNF217 played essential roles in host antibacterial immunity and inhibited the *Vibrio anguillarum* invasion into cells. Our study also found a microRNA miR-130-3p, which could inhibit antibacterial immune response and promote *V. anguillarum* invasion into cells by targeting NOD1. Moreover, we also found that the antibacterial effect inhibited by miR-130-3p could be reversed with circRNF217. In mechanism, our data revealed that circRNF217 was a competing endogenous RNA of NOD1 by sponging miR-130-3p, leading to activation of the NF-κB pathway and then enhancing the innate antibacterial responses. In addition, we also found that circRNF217 can promote the antiviral response caused by *Siniperca chuatsi* rhabdovirus through targeting NOD1. Our study provides new insights for understanding the impact of circRNA on host–pathogen interactions and formulating fish disease prevention to resist the severely harmful *V. anguillarum* infection. *The Journal of Immunology*, 2022, 208: 1099–1114.

The innate immune system, as the first barrier system in the evolution of the interaction between the host and pathogens, plays an important role in the elimination of foreign pathogens. Innate immunity mainly uses pattern recognition receptors (PRRs) to recognize the various pathogens' pathogen-associated molecular patterns (PAMPs) and initiate signal transduction (1, 2). The types of PAMP reported in existing studies include bacterial flagellin, LPS, viral dsRNA, and viral ssRNA (3). They are specifically recognized by PRRs to activate downstream signaling pathways and trigger antibacterial or antiviral responses. Nucleotide oligomer-like receptors are a kind of cytoplasmic PRR (4); among them, NOD1 was the first nucleotide oligomer-like receptor discovered, and it has been confirmed that it can recognize Gram-negative bacteria γ-D-glutamyl-meso-diaminopimelic acid and LPS, then recruit RIPK2 to activate the NF-κB signaling pathway to induce inflammation (5, 6). NOD1 is also found in teleost fish, unlike mammals, considering that most teleost fish lack TLR4, which can recognize LPS, or lack the MD2 and CD14 costimulatory molecules required for TLR4 recognition (7, 8). Therefore, the study of NOD1 is of great significance for determining the host's antibacterial immune response after bacterial infection in fish. In addition, recent studies have found that fish NOD1 can recognize viruses that invade host cells. After NOD1 recognizes the viral nucleic acid, it can recruit MAVS to activate the downstream NF-κB/IRF3 pathway to play an antiviral effect (9).

In recent years, people have discovered a series of regulatory factors involved in the regulation of the NOD1 signaling pathway, such as CENTB1 (10), HSP90 (11), and SGT1 (12), which directly regulate NOD1 and thus positively regulate the NOD1 signaling pathway. In addition to protein regulatory factors, RNA molecules have also been found to play an important regulatory role in the NOD1 signaling pathway in recent years. As a research hotspot in recent years, circular RNA (circRNA) was first proposed as a viroid RNA in 1976 (13). As a covalently closed RNA molecule (14), circRNA is considered to be a by-product of splicing abnormalities (15). Due to the lack of the special structure of 5′ cap and 3′ polyadenylic acid tail, circRNA is not easily degraded by RNase R and is more stable than its homologous linear mRNA, with a half-life of >48 h (16). Moreover, circRNA also has a certain degree of conservation in species. In recent years, with the rapid development of bioinformatics and high-throughput sequencing technology, research has mainly identified three types of circRNA (17): circular exon RNA (EcircRNA), circular intron RNA, and exon–intron

*Laboratory of Fish Molecular Immunology, College of Fisheries and Life Science, Shanghai Ocean University, Shanghai, China; †Laboratory of Marine Biology and Biotechnology, Qingdao National Laboratory for Marine Science and Technology, Qingdao, China; ‡Key Laboratory of Exploration and Utilization of Aquatic Genetic Resources (Shanghai Ocean University), Ministry of Education, Shanghai, China; and §National Pathogen Collection Center for Aquatic Animals, Shanghai Ocean University, Shanghai, China

[1]W.Z. and H.S. contributed equally to this work.

ORCIDs: 0000-0002-2864-7055 (W.Z.); 0000-0001-9584-3294 (H.S.); 0000-0002-8389-020X (X.L.); 0000-0003-3606-8069 (T.X.).

Received for publication September 13, 2021. Accepted for publication December 24, 2021.

This work was supported by the National Natural Science Foundation of China (31822057) and National Key Research and Development Project (2018YFD0900503).

The sequencing data presented in this article have been submitted to GenBank (https://www.ncbi.nlm.nih.gov/nuccore/MZ695829.1/) under accession number MZ695829.

Address correspondence and reprint requests to Dr. Tianjun Xu, Laboratory of Fish Molecular Immunology, College of Fisheries and Life Science, Shanghai Ocean University, Shanghai, China. E-mail address: tianjunxu@163.com

The online version of this article contains supplemental material.

Abbreviations used in this article: Ago2, Argonaute; ceRNA, competing endogenous RNA; circRNA, circular RNA; EcircRNA, circular exon RNA; EIcircRNA, exon–intron circular RNA; EPC, epithelioma papulosum cyprini cell; gDNA, genomic DNA; ISG, IFN-stimulating gene; MIC, *M. miiuy* intestine cell; MKC, *M. miiuy* kidney cell; MOI, multiplicity of infection; mut, sequence mutated in the miR-130-3p binding site; ncRNA, noncoding RNA; oe-circ, overexpression of circRNF217; PAMP, pathogen-associated molecular pattern; PRR, pattern recognition receptor; qPCR, quantitative PCR; RIP, RNA immunoprecipitation assay; SCRV, *Siniperca chuatsi* rhabdovirus; siRNA, small interfering RNA; UTR, untranslated region; wt, wild-type circRNF217 sequence; YFP, yellow fluorescent protein.

circRNA (EIcircRNA). Research on its function has found that most circRNAs can act as miRNA sponges (18); some circRNAs regulate gene expression at the level of transcription and splicing (19) or interact with RNA binding proteins (20); and a few circRNAs have translational functions (21). However, this research shows that there are many studies on EcircRNA, but there are still very few studies on EIcircRNA, especially in lower vertebrates, such as teleost fish.

MicroRNA (miRNA), as the most frequently studied noncoding RNA (ncRNA) molecule, uses its "seed region" to bind to the 3′ untranslated region (UTR) of mRNA to degrade mRNA, or to block its translation by base-pairing with target gene transcripts (22). miRNA also plays an important role in the regulation of the NOD1-mediated signaling pathway. For example, microRNA-495 inhibits high-glucose-induced inflammation of cardiac fibroblasts by regulating NOD1 in humans (23). Moreover, PPARγ-regulated miR-125a could target NOD1 and regulate NOD1-mediated angiogenesis (24). Because NOD1 is an important intracellular receptor that recognizes LPS in fish, the elucidation of the regulatory mechanism of the NOD1 signaling pathway in fish is even more important. Our laboratory had found that miR-144 and miR-217-5p can target and negatively regulate the expression of NOD1 to attenuate the NOD1-mediated inflammatory response in fish (25). Although there have been many reports on the regulation of NOD1 by small ncRNAs, it is particularly unknown whether there are other types of ncRNA that regulate NOD1-mediated immune response, especially circRNA.

Fish, as an important initial link in vertebrate evolution, has an innate immune system and adaptive immune system (26). Given that the molecular composition and functions of fish related to innate immunity are very similar to those of higher vertebrates when the host is invaded by a pathogen, a series of signals will be triggered to resist the invading pathogen (27). Therefore, fish can be used as a good biological model for immunological research, considering that the aquaculture industry is rapidly expanding while facing various pathogenic bacteria, such as *Vibrio anguillarum*, *Aeromonas hydrophila*, or *V. harveyi* (28, 29). Among them, *V. anguillarum* is the most lethal and widely spread pathogenic bacterium in the aquatic industry. It will cause huge economic losses to the aquatic industry every year (29–31). However, at present, there is still very little research on pathogenic bacteria proliferation regulation in aquaculture, and various relevant infection mechanisms and prevention and control strategies are not perfect, especially the research and coping strategies of *V. anguillarum*, so in-depth research is urgent.

In this study, we identify a competing endogenous RNA (ceRNA) regulatory network involved in antibacterial responses in teleost fish, miiuy croaker (*Miichthys miiuy*). We elaborate that fish NOD1 contributes to antibacterial immunity following the infection of *V. anguillarum*, which we found could prevent *V. anguillarum* from invading fish cells. Here, we have found that miR-130-3p target NOD1 and suppress NOD1-mediated antibacterial responses, thereby promoting *V. anguillarum* invasion into cells. Furthermore, our study suggests that an EIcircRNA, namely, circRNA RNF217 (circRNF217), can serve as a ceRNA for miR-130-3p to facilitate NOD1 expression, thereby modulating NOD1-mediated antibacterial responses and suppressing *V. anguillarum* invasion into cells. In addition, we found that circRNF217 can also weaken the inhibitory effect of miR-130-3p on NOD1 through the ceRNA mechanism, so as to promote NOD1 to inhibit the replication of *Siniperca chuatsi* rhabdovirus (SCRV) virus and enhance the antiviral immune response. To our knowledge, our results not only first elucidate the biological mechanism of the circRNA–miRNA–mRNA axis in antibacterial immune responses of fish but also provide newinsights for understanding the impact of circRNA on host–pathogen interactions and formulating fish disease prevention to resist the severely harmful *V. anguillarum* infection.

Materials and Methods

Ethics statement

All animal experimental procedures were performed in accordance with the National Institutes of Health's *Guide for the Care and Use of Laboratory Animals*, and the experimental protocols were approved by the Research Ethics Committee of Shanghai Ocean University (no. SHOU-DW-2018-047).

Sample and challenge

Miiuy croaker (~50 g) were obtained from Zhoushan Fisheries Research Institute, Zhejiang Province, China. Fish were acclimated in aerated seawater tanks at 25°C for 6 weeks before experiments. Experimental procedures and *V. anguillarum* infection or LPS treatment were performed as described previously (28, 32).

Sequencing analysis and circRNA identification

The spleen tissues from three healthy fish and three LPS-challenged fish were separated, and total RNAs were extracted for the construction of the cDNA library. Afterward, the cDNA libraries were sequenced using the Illumina HiSeq 2500 platform. The sequencing data have been deposited in the Sequence Read Archive (SRA) at the National Center for Biotechnology Information (NCBI) under accession number PRJNA691457 (https://www.ncbi.nlm.nih.gov/bioproject/PRJNA691457). Clean reads were aligned against the miiuy croaker reference genome using the mapping program TopHat2 (33). The unmapped reads were extracted and further aligned with miiuy croaker reference sequence by TopHat-fusion software (34). The junction reads with noncolinear ordering alignment on the same chromosome were regarded as candidate back-spliced junction reads. The back-spliced junction reads were used for the identification of circRNAs by CIRI software (35).

Cell culture and treatment

M. miiuy spinal marrow cells, *M. miiuy* kidney cells (MKCs), *M. miiuy* muscle cells, *M. miiuy* intestine cells (MICs), *M. miiuy* liver cells, *M. miiuy* brain cells, and MKCs were cultured in L-15 medium (HyClone) supplemented with 15% FBS (Life Technologies), 100 U/ml penicillin, and 100 μg/ml streptomycin at 26°C. Epithelioma papulosum cyprini cells (EPCs) were maintained in medium 199 (Invitrogen) supplemented with 10% FBS, 100 U/ml penicillin, and 100 mg/ml streptomycin at 28°C in 5% CO_2. For stimulation experiments, MKCs were challenged with *V. anguillarum* at a multiplicity of infection (MOI) of 10 and harvested at different times for RNA extraction. For stimulation experiments, MKCs and MICs were challenged with SCRV at a MOI of 5 and harvested at different times for RNA extraction. SCRV virus was isolated as described previously (36), and the replication of SCRV was detected by quantitative PCR (qPCR).

Plasmids construction

To construct the NOD1-3′ UTR reporter vector, we amplified the 3′ UTR of *M. miiuy* NOD1 gene, as well as *Sciaenops ocellatus* and *N. diacanthus* NOD1-3′ UTR, using PCR and cloned into pmirGLO luciferase reporter vector (Promega). Meanwhile, the sequences of *M. miiuy* NOD1-3′ UTR were inserted into the mVenus-C1 vector (Invitrogen), which included the sequence of enhanced GFP. To construct the circRNF217 overexpression vector, we amplified the full-length circRNF217 cDNA by specific primer pairs and cloned into pLC5-circ vector (Geneseed Biotech), which contained a front and back circular frame to promote RNA circularization. Also, the circRNF217 overexpression vectors of *S. ocellatus* and *N. diacanthus* were constructed by synthesizing the full-length circRNF217 cDNA of *S. ocellatus* and *N. diacanthus*, respectively. The empty vector with no circRNF217 sequence was used as a negative control. The mutated forms with point mutations in the miR-130-3p binding site were synthesized using Mut Express II Fast Mutagenesis Kit V2 with specific primers. The miR-130-3p sensor was created by inserting two consecutive miR-130-3p complementary sequences into psiCHECK vector (Promega). The correct construction of the plasmids was verified by Sanger sequencing and extracted through Endo-Free Plasmid DNA Miniprep Kit (Tiangen Biotech). To build pLC5-MS2, we inserted the MS2 fragment into the pLC5-circ vector and then inserted the MS2 sequence into any position in the circRNF217 sequence in the pLC5-circRNF217 vector, except for the binding site of miR-130-3p. The sequences of all primers are listed in Supplemental Table I.

RNA oligoribonucleotides

The miR-130-3p mimics are synthetic dsRNAs with stimulating naturally occurring mature miRNAs. The miR-130-3p mimics sequence was 5′-CAGUGCAAUAUUAAAAGGGCAU-3′. The miR-130-3p mimics mutant sequence was 5′-CGUGUAGGUAUUAAAAGGGCAU-3′. The negative control mimics sequence was 5′-UUCUCCGAACGUGUCACGUTT-3′. miRNA inhibitors are synthetic ssRNAs that sequester intracellular miRNAs

and block their activity in the RNA interfering pathway. The miR-130-3p inhibitors sequence was 5′-AUGCCCUUUUAAUAUUGCACUG-3′. The negative control inhibitors sequence was 5′-CAGUACUUUUGUGUAGUACAA-3′. The RNA interference sequences for circRNF217 are as follows: si-circRNF217-1 sequence, 5′-GGCUACUCGCACCCGCAGATT-3′; and si-circRNF217-2 sequence, 5′-UACUCGCACCCGCAGACAGTT-3. The scrambled control RNA sequence was 5′- GGCUACUCGCACGACUCAGTT-3′.

Cell transfection

Transient transfection of cells with miRNA mimic, miRNA inhibitor, or small interfering RNA (siRNA) was performed in 24-well plates using Lipofectamine RNAiMAX (Invitrogen), and transfection of cells with DNA plasmids was performed using Lipofectamine 3000 (Invitrogen) according to the manufacturer's instructions. For functional analyses, the overexpression plasmid (500 ng/well) or control vector (500 ng/well) and miRNA mimics (100 nM), miRNA inhibitor (100 nM), or siRNA (100 nM) were transfected into cells in culture medium and then harvested for further detection. For luciferase experiments, miRNA mimics (100 nM) or miRNA inhibitor (100 nM) and pmirGLO (500 ng/well) containing the wild or mutated plasmid of NOD1-3′ UTR were transfected into cells.

Bacteria invasion

V. anguillarum was washed with fresh medium three times, centrifuged, and diluted with fresh medium containing 100 μM FITC-D-Lys (Xiamen Bioluminor Bio-Technology). After 30 min of incubation at 37°C, the cells were centrifuged, washed with fresh medium three times, and then resuspended in PBS. MKCs or MICs (1×10^5 cells/well) were distributed in a 96-well plate and cultured in L-15 medium (HyClone) supplemented with 15% FBS (Life Technologies), 100 U/ml penicillin, and 100 μg/ml streptomycin at 26°C. Cells were grown to 60–70% confluence and then synchronized by serum starvation overnight. Then the cells were washed three times with PBS. FITC-labeled *V. anguillarum* (1×10^6 cells/ml) was added to the dishes in 200 μl of serum-free L-15 medium, which was allowed to infect MKCs or MICs at different times for invasion. The infected cells were washed three times with PBS, and 200 μl of L-15 medium supplemented with 15% FBS (Life Technologies), 100 U/ml penicillin, and 100 μg/ml streptomycin was added at 26°C for 1 h. Then the infected cells were washed three times with PBS and immobilized by incubating with 0.2% Triton X-100 in 4% paraformaldehyde for 30 min at room temperature. After DAPI staining (Beyotime), the cells were photographed and counted under a Leica DMiL8 fluorescence microscope and evaluated by using a Thermo Scientific Varioskan LUX. These experiments were repeated three times (J. Shu et al., manuscript posted on Research Square, DOI: https://doi.org/10.21203/rs.3.rs-221122/v2).

MKCs or MICs (1×10^5 cells/well) were distributed in a 96-well plate and cultured in L-15 medium (HyClone) supplemented with 15% FBS (Life Technologies), 100 U/ml penicillin, and 100 μg/ml streptomycin at 26°C. Cells were grown to 60–70% confluence and then synchronized by serum starvation overnight. Then the cells were washed three times with PBS. *V. anguillarum* (1×10^6 cells/ml) was added to the dishes in 200 μl serum-free L-15 medium, which was allowed to infect MKCs or MICs at different times for invasion. The infected cells were washed three times with PBS, and 200 μl of L-15 medium supplemented with 15% FBS (Life Technologies), 100 U/ml penicillin, and 100 μg/ml streptomycin was added at 26°C for 1 h. Then the infected cells were washed three times with PBS, 1 ml sterile ddH_2O was added, and the cells were lysed at 4°C for 30 min. Then the above cell lysate was diluted 1000 times and coated on the agar plates. The plates were incubated at 37°C for 12 h, and the colonies that emerged on the plates were counted.

Bacterial growth curve

The *V. anguillarum* suspension and the supernatant of MICs transfected with pcDNA3.1 and NOD1 or pLC5-circ and circRNF217 expression plasmids for 48 h were mixed in the ratio of 4:1. Then the *V. anguillarum* suspension was inoculated in Luria–Bertani medium to 1×10^5 CFUs/ml in 96-well plates (100 μl/well). The plates were incubated at 37°C, and bacterial growth was determined by measuring OD_{600} at every hour.

RNA extract and quantitative real-time PCR

For the isolation and purification of both cytoplasmic and nuclear RNA from MKCs, the Cytoplasmic & Nuclear RNA Purification Kit has been used according to the manufacturer's instructions (Norgen Biotek). Total RNA was isolated with TRIzol Reagent (Invitrogen), and the cDNA was synthesized using the FastQuant RT Kit (Tiangen), which includes DNase treatment of RNA to eliminate genomic contamination. The expression patterns of each gene were performed by using SYBR Premix Ex Taq (Takara). The small RNA was extracted by using miRcute miRNA Isolation Kit (Tiangen), and miRcute miRNA First Strand cDNA Synthesis Kit (Tiangen) was applied to reverse transcription of miRNAs. The expression analysis of miR-130-3p was executed by using the miRcute miRNA qPCR Detection Kit (Tiangen). Real-time PCR was performed in an Applied Biosystems QuantStudio 3 (Thermo Fisher Scientific). GAPDH and 5.8S rRNA were employed as endogenous controls for mRNA and miRNA, respectively. Primer sequences are displayed in Supplemental Table I.

Luciferase reporter assay

The wild-type of circRNF217 and the mutant devoid of the miR-130-3p binding site were cotransfected with miR-130-3p mimics into EPCs. At 48 h posttransfection, reporter luciferase activities were measured using the dual-luciferase reporter assay system (Promega). To determine the functional regulation of circRNF217, we cotransfected cells NOD1 overexpression plasmid or circRNF217 overexpression plasmid, together with NF-κB, IL-1β, IRSE, and IRF3 luciferase reporter gene plasmids, phRL-TK *Renilla* luciferase plasmid, and either miR-130-3p mimics or negative controls. At 48 h posttransfection, the cells were lysed for reporter activity using the dual-luciferase reporter assay system (Promega). The miR-130-3p sensor was cotransfected with miR-130-3p mimics or circRNF217 overexpression plasmid. At 48 h posttransfection, the cells were lysed for reporter activity. All the luciferase activity values were achieved against the *Renilla* luciferase control. Transfection of each construct was performed in triplicate in each assay. Ratios of *Renilla* luciferase readings to firefly luciferase readings were taken for each experiment, and triplicates were averaged.

Western blotting

Cellular lysates were generated by using 1× SDS-PAGE loading buffer. Proteins were extracted from cells and measured with the BCA Protein Assay kit (Vazyme), then subjected to SDS-PAGE (8%) gel and transferred to polyvinylidene difluoride (Millipore) membranes by semidry blotting (Bio-Rad Trans Blot Turbo System). The membranes were blocked with 5% BSA. Protein was blotted with different Abs. The Ab against NOD1 was diluted at 1:500 (Abcam), anti-Flag and anti-Tubulin mAbs were diluted at 1:2000 (Sigma), and the HRP-conjugated anti-rabbit IgG or anti-mouse IgG (Abbkine) was diluted at 1:5000. The results were representative of three independent experiments. The immunoreactive proteins were detected by using WesternBright ECL (Advansta). The digital imaging was performed with a cold charge-coupled device camera.

RNase R treatment

The RNAs (10 μg) from MKCs were treated with RNase R (3 U/μg; Epicenter) and incubated for 30 min at 37°C. Then the treated RNAs were reverse transcribed with divergent primer or convergent primer and detected by qPCR and RT-PCR assay followed by nucleic acid electrophoresis.

Nucleic acid electrophoresis

The cDNA and genomic DNA (gDNA) PCR products were investigated using 2% agarose gel electrophoresis with Tris-acetate-EDTA running buffer. DNA was separated by electrophoresis at 100 V for 30 min. The DNA marker was Super DNA Marker (100–10,000 bp) (CWBIO). The bands were examined by UV irradiation.

RNA pull-down assay

circRNF217 and circRNF217-mut with mutated miR-130-3p binding sites were transcribed in vitro. The two transcripts were biotin labeled with the T7 RNA polymerase and Biotin RNA Labeling Mix (Roche), treated with RNase-free Dnase I, and purified with the RNeasy Mini Kit (Qiagen). The whole-cell lysates from MKCs ($\sim 1.0 \times 10^7$) were incubated with purified biotinylated transcripts for 1 h at 25°C. The complexes were isolated by streptavidin agarose beads (Invitrogen). RNA was extracted from the remaining beads, and qPCR was used to evaluate the expression levels of miRNAs.

To conduct pull-down assay with biotinylated miRNA, we harvested MKCs at 48 h after transfection, then incubated them on ice for 30 min in lysis buffer (20 mM Tris [pH 7.5], 200 mM NaCl, 2.5 mM $MgCl_2$, 1 mM DTT, 60 U/ml Superbase-In, 0.05% Igepal, protease inhibitors). The lysates were precleared by centrifugation for 5 min, and 50 μl of the sample was aliquoted for input. The remaining lysates were incubated with M-280 streptavidin magnetic beads (Sigma). To prevent the nonspecific binding of RNA and protein complexes, we coated the beads with RNase-free BSA and yeast tRNA (both from Sigma). The beads were incubated for 4 h at 4°C, washed twice with ice-cold lysis buffer, three times with the low-salt buffer (0.1% SDS, 1% Triton X-100, 2 mM EDTA, 20 mM Tris–HCl [pH 8.0], and 150 mM NaCl), and once with the high-salt buffer (0.1% SDS, 1% Triton X-100, 2 mM EDTA, 20 mM Tris–HCl [pH 8.0], and 500 mM NaCl). RNA

was extracted from the remaining beads with TRIzol Reagent (Invitrogen) and evaluated by qPCR.

RNA immunoprecipitation assay

RNA immunoprecipitation assay (RIP) experiments were performed by using the Magna RIP RNA-Binding Protein Immunoprecipitation Kit (Millipore) following the manufacturer's protocol. The Ago-RIP assay was conducted in MKCs (~2.0×10^7) transfected with Argonaute (Ago2)-flag or pcDNA3.1-flag and miR-130-3p mimics or control mimics. After 48-h transfection, the cells were extracted and incubated with magnetic beads conjugated with IgG and anti-Flag Ab (Sigma). RNA was extracted from the remaining beads, and qPCR was used to evaluate the expression levels of circRNF217. The MS2-RIP assay was also conducted in MKCs (~2.0×10^7) transfected with pLC5-MS2, pLC5-MS2-circRNF217, pLC5-MS2-circRNF217-mut, or pLC5-MS2-GFP (Addgene). PLC5-MS2-GFP plasmid can express GFP protein and can be detected by anti-GFP Ab (Abcam). After 48-h transfection, the MKCs were used in RIP assays via the Magna RIP RNA-Binding Protein Immunoprecipitation Kit (Millipore) and an anti-GFP Ab following the manufacturer's protocol. RNA was extracted from the remaining beads, and qPCR was used to evaluate the expression levels of miRNAs.

Cell viability and EdU cell proliferation assay

Cell viability was measured at 48 h after transfection in MKCs with CellTiter-Glo Luminescent Cell Viability assays (Promega) according to the manufacturer's instructions. The EdU assay was performed to assess the proliferation of cells by using the BeyoClick EdU cell Proliferation Kit with Alexa Fluor 555 (Beyotime) following the manufacturer's instructions. The EdU cell lines were photographed and counted under a Leica DMiL8 fluorescence microscope and evaluated by Thermo Scientific Varioskan LUX. These experiments were repeated three times.

Statistical analysis

Data are expressed as the mean ± SE from at least three independent triplicate experiments. The Student *t* test was used to evaluate the data. The relative gene expression data were acquired using the $2^{-\Delta\Delta CT}$ method, and comparisons between groups were analyzed by one-way ANOVA followed by Duncan multiple comparison tests (37). A p value <0.05 was considered significant.

Results

Characterization of circRNF217 involved in antibacterial immunity

Increasing pieces of studies have shown that circRNA can play a regulatory role as a spongy body adsorbing miRNA and interfere with the host's immune signaling pathways through the sponge mechanism. We treated miiuy croaker with LPS to identify where circRNAs are potentially involved in the regulation of infection, and then the expression of circRNAs in the spleen tissues of the treated group and the untreated group was analyzed by RNA sequencing data. We found that a highly expressed circRNA (named circRNF217) is copresent in the differentially expressed genes obtained after LPS treatment (Fig. 1A). To confirm the reliability of this result, we conducted in vivo and in vitro experiments to detect the changes in the expression level of *RNF217* and circRNF217 under *V. anguillarum* stimulation. The results of qPCR experiments showed that circRNF217 was significantly upregulated in miiuy croaker spleen tissue treated with *V. anguillarum* or LPS at different time points, but not *RNF217* (Fig. 1B, 1C). In addition, *V. anguillarum*–treated miiuy croaker kidney cells (MKCs) further confirmed the significant expression of circRNF217 and did not influence the expression of *RNF217* (Fig. 1D). We then evaluated the expression levels of circRNF217 in *M. miiuy* spinal marrow cells, *M. miiuy* muscle cells, MICs, *M. miiuy* liver cells, *M. miiuy* brain cells, and MKCs (Fig. 1E). Among the aforementioned cell lines, MKCs and MICs showed the highest and the lowest expression of circRNF217, respectively. Therefore, we selected MKCs and MICs to investigate the function and regulatory mechanism of circRNF217.

The transcriptome sequencing revealed that circRNF217 was 1626 bp in length (right panel of Fig. 1F). Using the miiuy croaker whole-genome library to perform blast analysis on the RNF217 gene, we found that the RNF217 gene was located on chromosome 19, which was composed of 12 exons, and circRNF217 was self-cyclized from exon2-exon5 and intron2-intron4. To confirm the objective existence of circRNF217, first, we designed circRNF217 divergent primers for RT-PCR amplification, and the amplified products were subjected to Sanger sequencing to confirm that circRNF217 was spliced from the head to the tail (left panel of Fig. 1F). Then we used convergent primers to amplify the *RNF217* gene (GenBank accession number MZ695829; https://www.ncbi.nlm.nih.gov/nuccore/MZ695829.1/) and divergent primers to amplify circRNF217. cDNA and gDNA were extracted separately from MKCs and MICs and subjected to RT-PCR and agarose gel electrophoresis assays. The results shown in Fig. 1G indicated that circRNF217 was amplified from cDNA by using only divergent primers, whereas no amplification product was observed from gDNA. Considering that stability was a crucial characteristic of circRNA, we thus used RNase R to confirm the stability of circRNF217. The results from the analysis of RT-PCR and agarose gel electrophoresis assay showed that circRNF217, rather than linear RNF217 or GAPDH, resisted digestion by RNase R (Fig. 1H). In addition, we detected the distribution of circRNF217 by cytoplasmic nuclear fractionation experiments and found that circRNF217 was primarily localized in the cytoplasm (Fig. 1I). Accordingly, these results suggested that circRNF217 was a stable circRNA expressed and primarily distributed in the cytoplasm.

circRNF217 enhances host antibacterial innate immunity

We designed two siRNAs against circRNF217, and the overexpression plasmid of circRNF217 was constructed to explore the biological function of circRNF217 (Fig. 2A, 2B). Consequently, two siRNAs (si-circRNF217-1 and si-circRNF217-2) evidently decreased the circRNF217 expression level, but such siRNAs did not affect the expression level of linear *RNF217* mRNA in MKCs. Because si-circRNF217-1 could induce higher inhibitory efficiency, we selected si-circRNF217-1 (si-circ) for the subsequent experiment (left panel of Fig. 2C). Moreover, the circRNF217 overexpression plasmid was successfully constructed, because it significantly increased the circRNF217 expression levels rather than linear *RNF217* mRNA in MKCs (right panel of Fig. 2C). Considering the important role of inflammatory cytokines in the clearance of invading bacteria, we focused on investigating the role of circRNF217 in regulating the expression of inflammatory cytokines. As shown in Fig. 2D, knockdown of circRNF217 (si-circ) could significantly inhibit the expression levels of TNF-α, IL-1β, and IL-8 after LPS treatment. In contrast, overexpression of circRNF217 (oe-circ) increased the expression levels of these genes under LPS treatment. We also found that knockdown of circRNF217 (si-circ) could significantly inhibit the expression levels of TNF-α, IL-1β, and IL-8 after *V. anguillarum* treatment (Fig. 2E), and oe-circ increased the expression levels of these genes under *V. anguillarum* treatment (Fig. 2F). Then, by labeling *V. anguillarum* with FITC-D-Lys, we found that *V. anguillarum* could invade MICs and MKCs (Supplemental Fig. 1, Fig. 2G). The results showed that knockdown of circRNF217 could significantly increase the *V. anguillarum* invading MKCs, and oe-circ decreased the *V. anguillarum* invading MICs (Fig. 2G). To further confirm the effect of circRNF217 on *V. anguillarum* invading cells, a plate counting method was used to confirm the number of *V. anguillarum* invading cells. The results showed that knockdown of circRNF217 could significantly increase the *V. anguillarum* invading MKCs (Fig. 2H), and oe-circ decreased the *V. anguillarum* invading MICs (Fig. 2I). We conducted EdU assays to examine the cell proliferation in MKCs and MICs and to explore the function of circRNF217 in antibacterial innate immunity. The results showed that knockdown of circRNF217 considerably decreased the percentages of

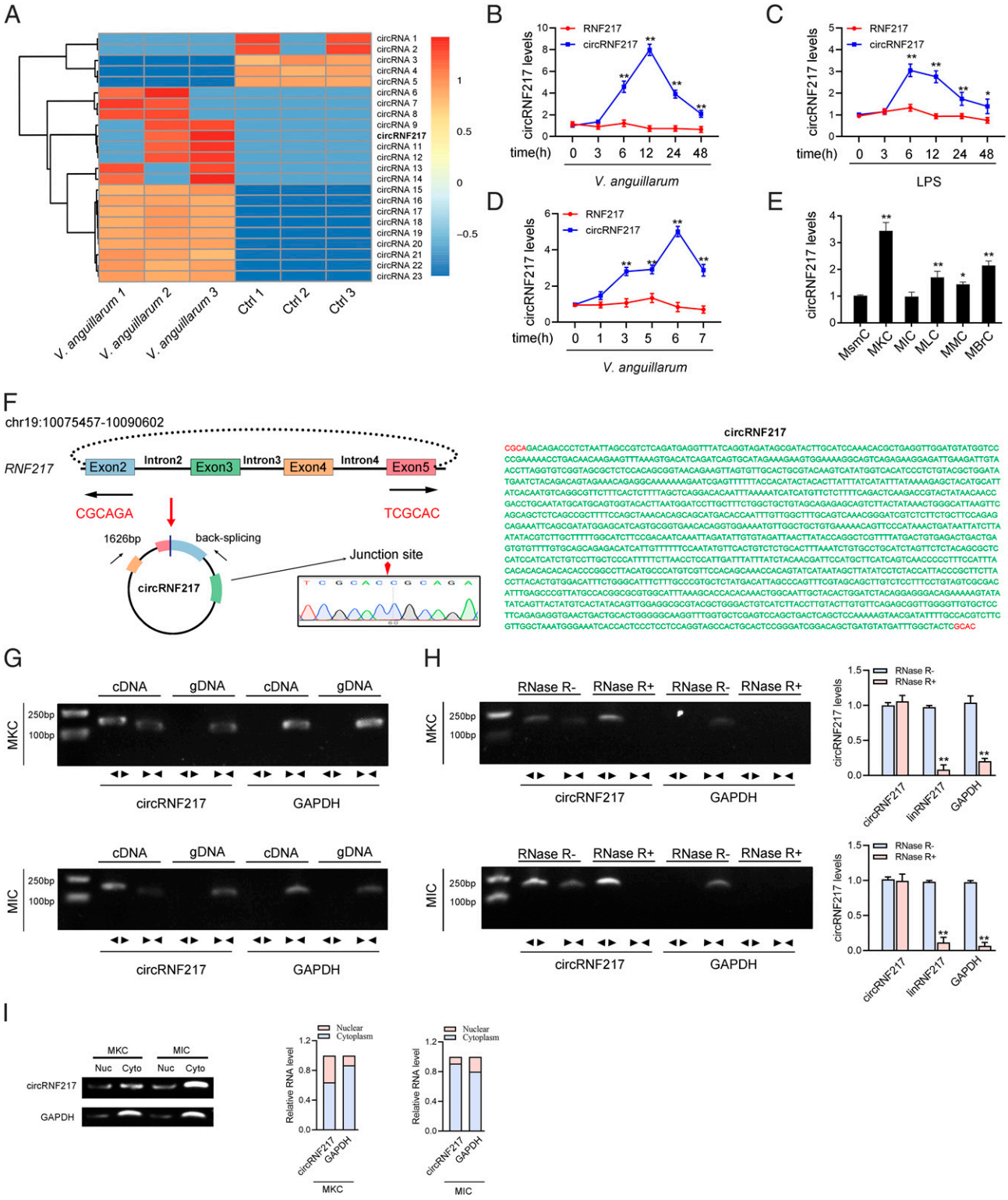

FIGURE 1. Expression profiles and characterization of circRNF217. (**A**) A cluster heatmap presented the significantly dysregulated circRNAs in *V. anguillarum*–treated spleen tissues compared with untreated tissues. The red and blue strips represented high and low expression, respectively. (**B**) The expression levels of *RNF217* and circRNF217 in spleen samples were measured by qRT-PCR at the indicated time after *V. anguillarum* infection. (**C**) The expression levels of *RNF217* and circRNF217 in spleen samples were measured by qRT-PCR at the indicated time after LPS treatment. (**D**) The expression levels of *RNF217* and circRNF217 in MKCs were measured by qRT-PCR at the indicated time after *V. anguillarum* infection. (**E**) Relative expression of circRNF217 in indicated cell lines was determined by qRT-PCR. (**F**) We confirmed the head-to-tail splicing of circRNF217 in the circRNF217 RT-PCR product by Sanger sequencing. (**G**) RT-PCR validated the existence of circRNF217 in MKC and MIC lines. circRNF217 was amplified by divergent primers in cDNA, but not gDNA. GAPDH was used as a negative control. (**H**) The expression of circRNF217 and linear *RNF217* mRNA in both MIC and MKC lines was detected by RT-PCR assay followed by nucleic acid electrophoresis or qPCR assay in the presence or absence of RNase R. (**I**) circRNF217 was mainly localized in the cytoplasm. RNA isolated from nuclear and cytoplasm was used to analyze the expression of circRNF217 by RT-PCR. Representative results are from three independent experiments, and statistical data are expressed as the mean ± SE. (A) $n = 3$ biological replicates; (B–I) $n = 3$ biological replicates × 3 technical replicates. $^{*}p < 0.05$, $^{**}p < 0.01$.

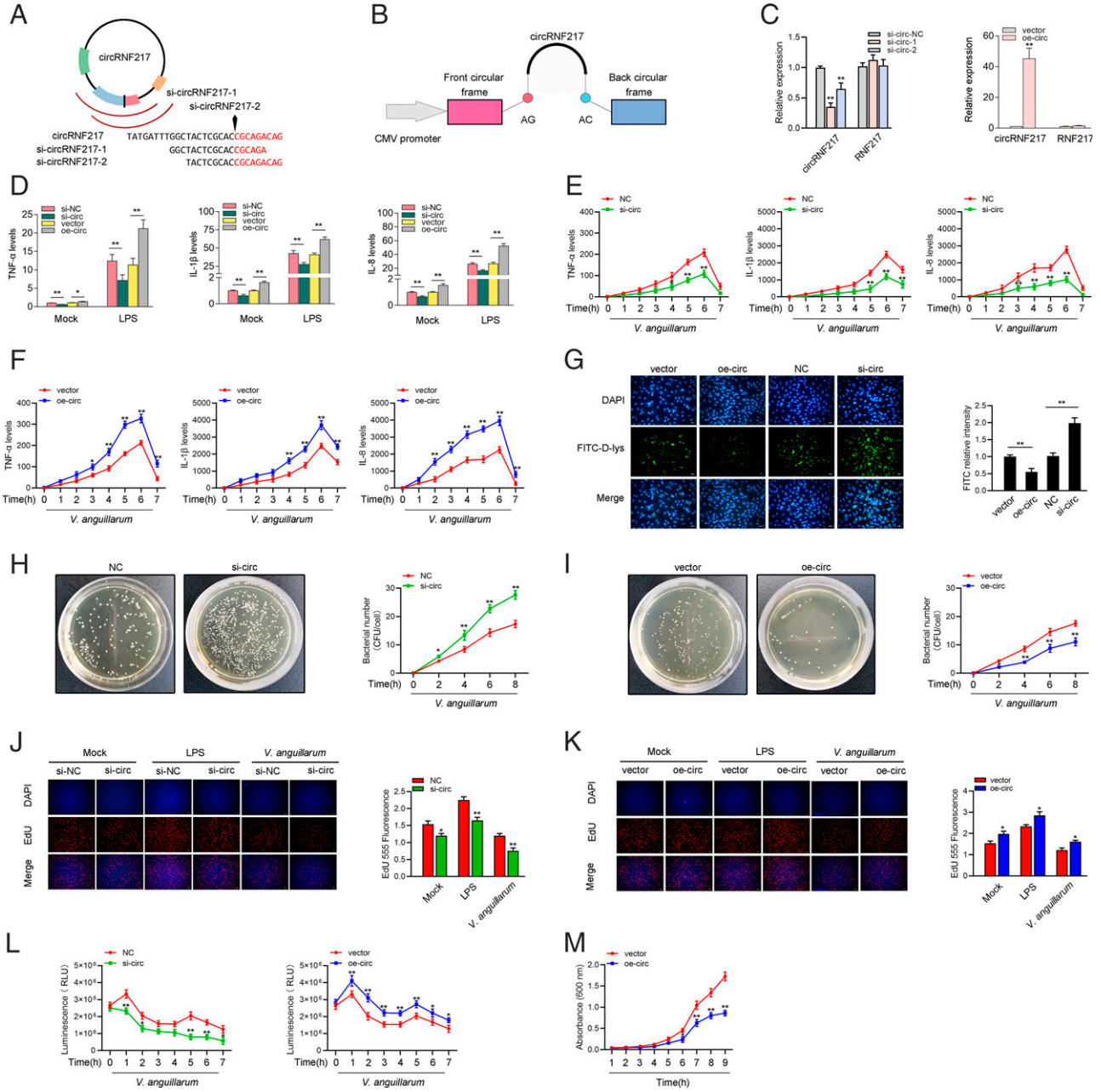

FIGURE 2. circRNF217 promotes antibacterial innate immunity. (**A** and **B**) The schematic of siRNAs (A) and oe-circ structure (B) qPCR analysis of circRNF217 and linear RNF217 mRNA in MKCs treated with siRNAs. (**C**) qPCR analysis of circRNF217 and linear RNF217 mRNA in MICs stably overexpressing circRNF217. (**D**) qPCR assays were performed to determine the expression levels of TNF-α, IL-1β, and IL-8 in MKCs transfected with overexpression plasmid (oe-circ) or control vector (pLC5-ciR) and transfected with (si-circRNF217-1) si-circ or NC after LPS treatment. (**E** and **F**) qPCR assays were performed to determine the expression levels of TNF-α, IL-1β, and IL-8 in MKCs transfected with si-circ or NC (E) and in MICs transfected with oe-circ or control vector (F) after *V. anguillarum* infection. (**G**) MICs were transfected with oe-circ or control vector and MKCs were transfected with si-circ or NC, then infected with FITC-labeled *V. anguillarum*, and then examined by using a fluorescence microscope. Scale bars, 20 μm; original magnification ×400. (**H** and **I**) MKCs were transfected with si-circ or NC (H) and MICs were transfected with oe-circ or control vector (I) and then infected with *V. anguillarum.* The intracellular bacterial number was determined at different hours postinfection and shown as CFUs. (**J** and **K**) Cell proliferation was assessed by EdU assays in MKCs transfected with si-circ or NC after LPS treatment for 12 h or *V. anguillarum* infection for 6 h (J) and in MICs transfected with oe-circ or vector after LPS treatment for 12 h or *V. anguillarum* infection for 6 h (K). Scale bars, 20 μm; original magnification ×200. (**L**) Effect of circRNF217 on cell viability after *V. anguillarum* infection. MKCs were transfected with si-circ or NC for 24 h, and MICs were transfected with pLC5-ciR vector or oe-circ for 24 h, then treated with *V. anguillarum* for different times. Cell viability assays were measured. (**M**) The *V. anguillarum* suspension and the supernatant of MICs transfected with vector and oe-circ expression plasmids for 48 h were mixed. Then the above *V. anguillarum* suspension in Luria–Bertani medium in 96-well plates was inoculated, the plates were incubated at 37°C, and bacterial growth was determined by measuring OD_{600} at different times. Representative results are from three independent experiments, and statistical data are expressed as mean ± SE. (C–F) $n = 3$ biological replicates × 3 technical replicates, (G) $n = 4$ biological replicates, (H and I) $n = 3$ biological replicates × 3 technical replicates, (J and K) $n = 3$ biological replicates, (L and M) $n = 3$ biological replicates × 3 technical replicates. *$p < 0.05$; **$p < 0.01$.

EdU-positive cells (Fig. 2J) but greatly increased with the oe-circ, suggesting that circRNF217 promoted the proliferation of miiuy croaker cell lines (Fig. 2K). When we investigated the effect of circRNF217 on cell viability of MKCs, we found that knockdown of circRNF217 significantly decreased cell viability compared with the control group after 1 and 5 h of *V. anguillarum* infection (left panel of Fig. 2L). Furthermore, we found that oe-circ significantly increased cell viability compared with the control group after 1 and 5 h of *V. anguillarum* infection (right panel of Fig. 2L). By measuring the growth curve of *V. anguillarum*, we found that the cell culture medium of MICs transfected with circRNF217 could inhibit the growth of *V. anguillarum*. In summary, these data indicate that circRNF217, as a positive regulator, is involved in the regulation of antibacterial immunity, and the date of the cell proliferation and viability suggest that circRNF217 can positively regulate the antibacterial responses and upregulate the expression of inflammatory cytokines, thus reducing *V. anguillarum* invading cells, promoting cell proliferation, and increasing cell viability.

circRNF217 is able to regulate miR-130-3p expression and activity

We examined the ability of circRNF217 to bind to miRNAs to explore whether circRNF217 can function as a miRNA sponge. To this end, we transfected Ago2-flag or pcDNA3.1-flag into MKCs to conduct RNA immunoprecipitation (RIP) for Ago2. The results showed that endogenous circRNF217 could be pulled down by Ago2-flag (Fig. 3A), indicating that circRNF217 might have a binding site with miRNA. After we found miRNAs combined with circRNF217, we used miRNA target prediction tools, including TargetScan, miRanda, and RNAhybrid for prediction, and selected six candidate miRNAs for further verification (Fig. 3B, 3C). Afterward, we compared the expression levels of these candidate miRNAs in MKCs transfected with si-circ or negative control and MICs transfected with overexpression plasmid (oe-circ) or control vector (vector). Among the six candidate miRNAs, miR-130-3p expression was significantly reduced when circRNF217 was overexpressed (Fig. 3D), whereas miR-130-3p expression was significantly enhanced in response to circRNF217 inhibition compared with other candidate miRNAs (Fig. 3E); we think it may be because miR-130-3p are adsorbed by circRNF217. We constructed the miR-130-3p sensor to detect whether circRNF217 affects the activity of miR-130-3p and to consolidate the direct binding of miR-130-3p and circRNF217. Then we transfected the miR-130-3p sensor with miR-130-3p, pLC5-ciR vector, or circRNF217 overexpression plasmid. The decreased luciferase activity induced by miR-130-3p was recovered when cotransfected with circRNF217 overexpression plasmid, suggesting that circRNF217 specifically sponged miR-130-3p, thereby preventing it from inhibiting luciferase activity (Fig. 3F). Collectively, circRNF217 could regulate miR-130-3p expression and activity, and circRNF217 might function as a sponge of miR-130-3p.

circRNF217 functions as a miRNA sponge of miR-130-3p

To investigate whether circRNF217 could directly bind miR-130-3p, we analyzed the sequences of circRNF217 and noted that circRNF217 possessed a complementary sequence to the miR-130-3p seed region (Fig. 4A). Next, Luciferase reporters were constructed by inserting

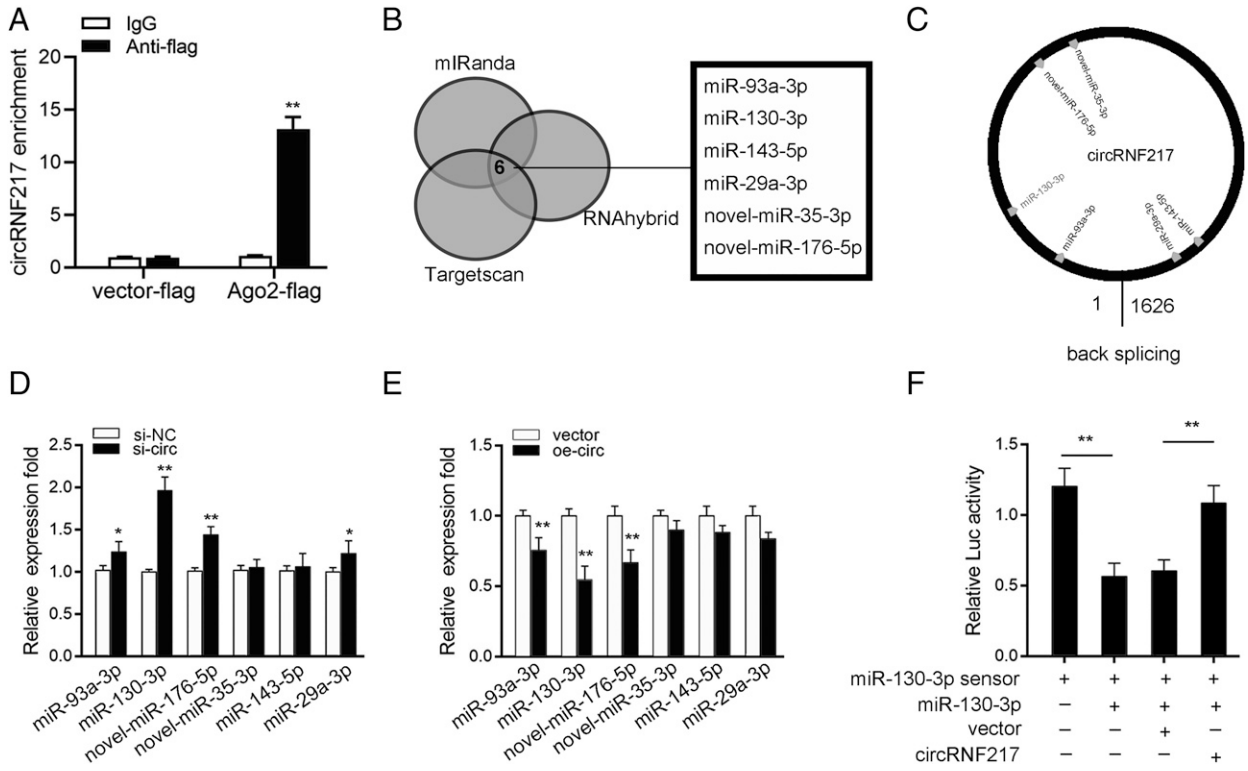

FIGURE 3. circRNF217 regulates miR-130-3p expression and activity. (**A**) The Ago2-RIP assay for the amount of circRNF217 in MICs transfected with Ago2-flag or pcDNA3.1-flag. (**B**) A schematic illustration showing overlapping of the target miRNAs of circRNF217 predicted by TargetScan, miRanda, and RNAhybrid. (**C**) Schematic drawing showing the putative binding sites of the miRNAs associated with circRNF217. (**D** and **E**) Relative expression of candidate miRNAs in MICs and MKCs transfected with oe-circ (D) and si-circ (E), respectively. (**F**) circRNF217 reduces miR-130-3p activity. The relative luciferase activity was analyzed in MKCs cotransfected with mimics, circRNF217 overexpression plasmid, and control vector, together with the miR-130-3p sensor. Representative results are from three independent experiments, and statistical data are expressed as mean ± SE. (A) $n = 3$ biological replicates × 3 technical replicates; (D–F) $n = 3$ biological replicates × 2 technical replicates. $^*p < 0.05$, $^{**}p < 0.01$.

either the wild-type circRNF217 sequence (wt) or the sequence mutated in the miR-130-3p binding site (mut) into the pmirGLO vector. Luciferase assays showed that upregulation of miR-130-3p could remarkably decrease the luciferase activities of the wild-type of circRNF217 reporter plasmid, but not the mutant (Fig. 4B). It was subsequently confirmed that miR-130-3p mimics inhibited luciferase activity in time-dependent ways (Fig. 4C). In addition, wild-type or a mutant type of circRNF217 sequence was inserted into mVenus-C1 vector and detected whether cotransfecting with miR-130-3p could suppress the levels of yellow fluorescent protein (YFP). The results revealed that miR-130-3p could significantly inhibit the levels of GFP (Fig. 4D, 4E), which suggested that a direct interaction might exist between circRNF217 and miR-130-3p.

Given that miRNAs inhibit translation and degrade mRNAs in an Ago2-depedent manner by binding to their targets, we further tested the ability of circRNF217 to bind to miR-130-3p. To this end, we conducted RIP assays in MKCs by cotransfecting Ago2-flag, miR-130-3p, and miR-130-3p-mut. The qPCR analysis results indicated that circRNF217 pulled down with Ago2-flag was markedly enriched when transfected with miR-130-3p mimics, but not miR-130-3p-mut (Fig. 4F). To further confirm the direct interaction between circRNF217 and miR-130-3p, we conducted RNA pull-down detected with biotin-labeled circRNF217 probe or biotin-labeled miR-130-3p. The qPCR analysis results revealed that miR-130-3p could be pulled down by biotin-labeled circRNF217, but not circRNF217-mut (Fig. 4G). In addition, biotin-labeled miR-130-3p captured more circRNF217 than the negative control, whereas the biotin-labeled mutant type of miR-130-3p did not (Fig. 4H). Furthermore, we cloned an MS2 fragment into pLC5 vector, pLC5-circRNF217, and pLC5-circRNF217-mut plasmids to construct plasmids capable of producing MS2 protein. In addition, we cotransfected pLC5-MS2-GFP plasmid, which can produce GFP-MS2 fusion protein that could bind with the MS2 fragment and be identified by anti-GFP Ab. Hence miRNAs interacting with circRNF217 could be pulled down by the GFP-MS2-circRNF217 compounds. The results from qPCR assays showed that miR-130-3p was

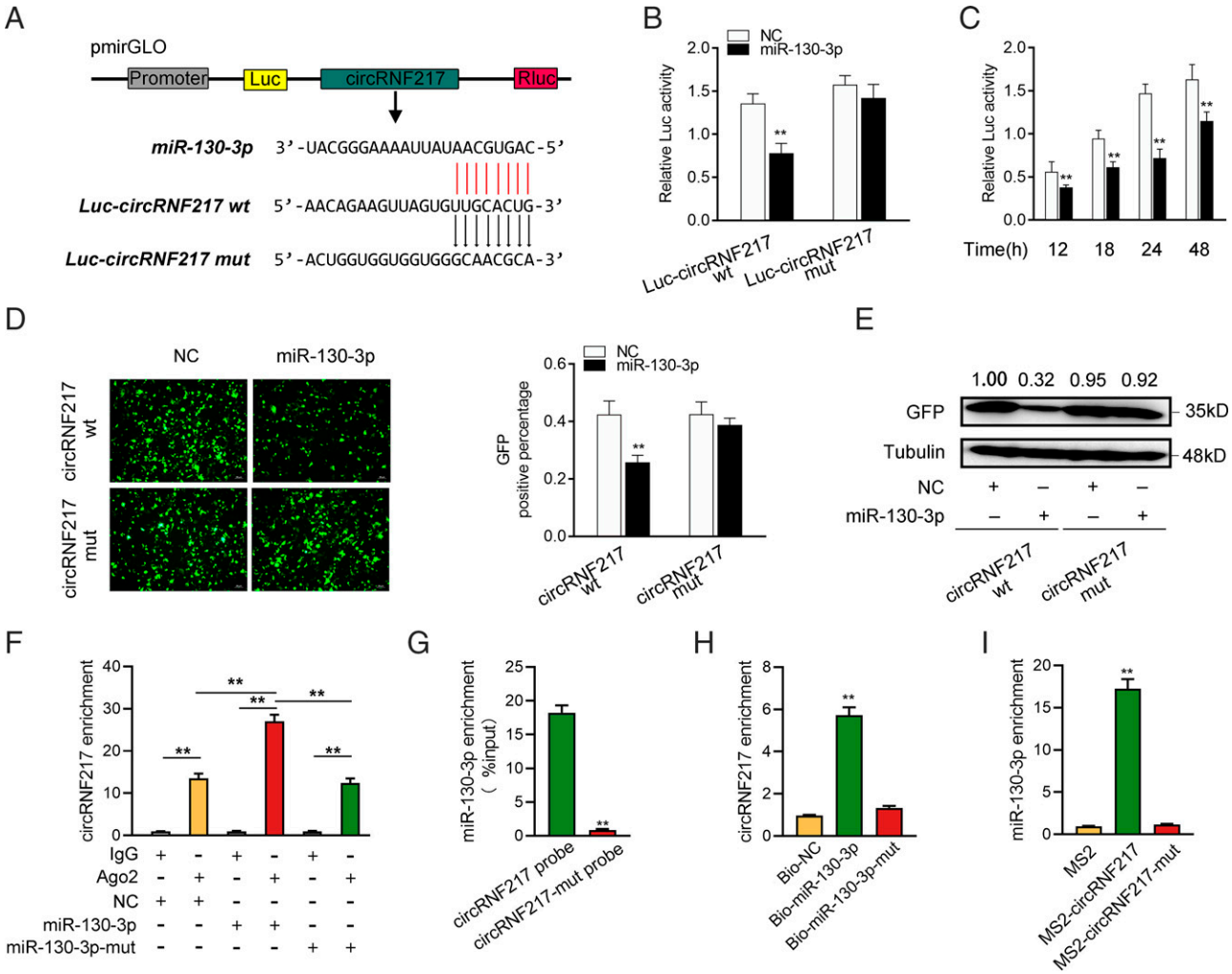

FIGURE 4. circRNF217 functions as a miRNA sponge of miR-130-3p. (**A**) Schematic illustration of circRNF217-wt and circRNF217-mut luciferase reporter vectors. (**B**) The relative luciferase activities were detected in EPCs after cotransfection with circRNF217-wt or circRNF217-mut and mimics or NC. (**C**) The time gradient experiment of miR-130-3p mimics was conducted. (**D** and **E**) circRNF217 downregulated YFP expression. EPCs were cotransfected with circRNF217-wt or circRNF217-mut and mimics or NC. The fluorescence intensity and the YFP expression were evaluated by enzyme-labeled instruments and Western blotting, respectively. Scale bars, 20 μm; original magnification ×200. (**F**) The Ago2-RIP assay was executed in MKCs after transfection with miR-130-3p, miR-130-3p-mut, and NC, followed by qPCR to detect cirRNF217 expression levels. (**G** and **H**) RNA pull-down assay was executed in MICs, followed by qPCR to detect the enrichment of circRNF217 and miR-130-3p. (**I**) The MS2-RIP assay was executed in MICs after transfection with pLC5-circ-MS2, pLC5-MS2-circRNF217, and pLC5-MS2-circRNF217-mut, followed by qPCR to detect the enrichment of miR-130-3p. Representative results are from three independent experiments, and statistical data are expressed as mean ± SE. (B and C) $n = 3$ biological replicates × 2 technical replicates, (D and E) $n = 3$ biological replicates, and (F–I) $n = 3$ biological replicates × 3 technical replicates. $^{**}p < 0.01$.

significantly enriched for pLC5-circRNF217 compared with pLC5-circRNF217-mut or empty vector (Fig. 4I). Collectively, these data suggest that circRNF217 can directly bind to miR-130-3p, and circRNF217 acts as a sponge of miR-130-3p.

Fish NOD1 enhances antibacterial responses on V. anguillarum *infection*

Bacterial infection triggers host innate immune responses by activating transcription factors, namely, NF-κB, which coordinately induce the production of inflammatory cytokines. In investigating the fish NOD1-mediated signaling pathway in response to bacterial infection, we first examined the expression patterns of fish NOD1 on *V. anguillarum*. To this end, we treated MICs with *V. anguillarum* infection. During *V. anguillarum* infection, the expression levels of NOD1 were significantly increased (Fig. 5A). We silenced NOD1 and examined the expression patterns of indicated genes to confirm whether fish NOD1 is required for the induction of inflammatory cytokines on *V. anguillarum* infection. Knockdown of NOD1 effectively inhibited NOD1 expression at protein and mRNA levels (Fig. 5B).

Considering the important role of inflammatory cytokines in the clearance of invading bacteria, we focused on investigating the role of NOD1 in regulating the expression of inflammatory cytokines. As shown in Fig. 5C, knockdown of NOD1 could significantly inhibit the expression levels of TNF-α, IL-1β, and IL-8 after *V. anguillarum* treatment. The results indicated that overexpression of NOD1 could decrease *V. anguillarum* invading cells, whereas NOD1-specific siRNA could increase the invasion of *V. anguillarum* into cells by silencing the expression of endogenous NOD1 (Fig. 5D). To further confirm the effect of NOD1 on *V. anguillarum* invading cells, we used the plate counting method to confirm the number of *V. anguillarum* invading cells. The results showed that knockdown of NOD1 could significantly increase the *V. anguillarum* invading MKCs (Fig. 5E), whereas overexpression of NOD1 decreased them (Fig. 5F). This result indicated the contribution of NOD1 to fish antibacterial responses in response to bacterial infection. We used NOD1-specific siRNA for further experiments to determine whether NOD1 can affect cell proliferation and viability on *V. anguillarum* infection. As shown in Fig. 5G and 5H, knockdown of NOD1 led to decreased cell viability in MKCs, as indicated by luminescent cell viability assay (Fig. 5G). The overexpression of NOD1 led to an increase in cell viability in MICs (Fig. 5H). By measuring the growth curve of *V. anguillarum*, we found that the cell culture medium of MICs transfected with NOD1 could inhibit the growth of *V. anguillarum*. Collectively, these data showed that fish NOD1 could mediate the activation of NF-κB. In addition, suppression of fish NOD1 expression could block inflammatory cytokines, reduce *V. anguillarum* invasion, and inhibit cell proliferation.

miR-130-3p suppresses antibacterial responses by targeting NOD1

We predicted the potential target genes of miR-130-3p by miRNA prediction programs, including TargetScan, miRanda, and MicroInspector (Fig. 6A) (38, 39). Among all possible target genes, we selected NOD1, a gene related to antibacterial immune responses, which is the PRR found to recognize LPS in teleost fish (8, 9). Therefore, we investigated whether NOD1 is the direct target gene of miR-130-3p. Prediction analysis showed that NOD1 contained the standard target sequence of miR-130-3p at the nucleotide of its 3′ UTR (Fig. 6B). To obtain evidence that NOD1-3′ UTR is the target of miR-130-3p, we integrated the NOD1-3′ UTR containing the target sequence or target site mutation fragment into the luciferase reporter vector (Fig. 6B). We cotransfected luciferase reporter plasmid with miR-130-3p mimics into EPCs. As shown in Fig. 6C, miR-130-3p mimics the significantly reduced luciferase activity of transfected wild-type NOD1-3′ UTR cells, but the luciferase activity of transfected mutant NOD1-3′ UTR cells had no effect. For further verification, wild-type or mutant NOD1-3′ UTR was inserted into the mVenus-C1 vector to investigate whether miR-130-3p mimics can inhibit the expression of YFP. As shown in Fig. 6D, compared with the transfection control mimic, miR-130-3p can significantly suppress YFP expression, while the fluorescence intensity of the cells transfected with the mutant NOD1-3′ UTR is unchanged. We transfected miR-130-3p mimics and inhibitors into MICs to test whether miR-130-3p participates in the regulation of NOD1 expression. The results from Western blotting and qRT-PCR assays results indicated that transfection of miR-130-3p mimics suppressed the expression levels of NOD1, whereas miR-130-3p inhibitors markedly enhanced the expression levels of NOD1 (Fig. 6E, 6F). Considering that miR-130-3p targets NOD1 and regulates its expression, we wanted to test whether NOD1-mediated activation of NF-κB and IRF3 signaling pathways is regulated by miR-130-3p. The results showed that the activation of NF-κB, IL-1β, ISRE, and IRF3 luciferase reporter genes was impeded by miR-130-3p mimics (Fig. 6G).

The results of qPCR experiments showed that miR-130-3p was significantly upregulated in miiuy croaker spleen tissue treated with LPS or *V. anguillarum* at different time points (Fig. 6H). In addition, LPS or *V. anguillarum*–treated miiuy croaker kidney cells (MKCs) further confirmed the significant expression of miR-130-3p (Fig. 6I). Then, we investigated the role of miR-130-3p in regulating TNF-α, IL-1β, and IL-8 to explore the biological function of miR-130-3p. To this end, we measured the effects of synthetic miR-130-3p mimics and inhibitors on the expression of miR-130-3p, and the results indicated that miR-130-3p mimics enhanced miR-130-3p expression sharply, whereas miR-130-3p inhibitors decreased miR-130-3p expression (Fig. 6J). Moreover, the results showed that TNF-α, IL-1β, and IL-8 were significantly decreased by the introduction of miR-130-3p mimics on LPS infection. In contrast, the inhibition of endogenous miR-130-3p significantly increased this elevated gene expression compared with transfection of control inhibitors (Fig. 6K). Meanwhile, the results also showed that TNF-α, IL-1β, and IL-8 were significantly decreased by the introduction of miR-130-3p mimics on *V. anguillarum* infection (Fig. 6L). On the contrary, the inhibition of endogenous miR-130-3p significantly increased the elevation of these gene expressions compared with transfection of control inhibitors (Fig. 6M). The results indicated that overexpression of miR-130-3p could increase *V. anguillarum* invading cells, whereas miR-130-3p inhibitor could decrease the invasion of *V. anguillarum* into cells (Fig. 6N). To further confirm the effect of miR-130-3p on *V. anguillarum* invading cells, we used a plate counting method to confirm the number of *V. anguillarum* invading cells. The results showed that miR-130-3p could significantly increase the *V. anguillarum* invading MKCs, and inhibition of miR-130-3p expression decreased the *V. anguillarum* invading MICs (Fig. 6O). We conducted EdU assays to examine the cell proliferation in MKCs and MICs and to explore the function of miR-130-3p in antibacterial innate immunity. The results showed that miR-130-3p considerably decreased the percentages of EdU-positive cells (Fig. 6P), but these percentages greatly increased with the inhibition of miR-130-3p expression, suggesting that miR-130-3p promoted the proliferation of miiuy croaker cell lines (Fig. 6Q). When we investigated the effect of miR-130-3p on cell viability of MKCs, we found that miR-130-3p significantly decreased cell viability compared with the control group after 1 and 5 h of *V. anguillarum* infection (left panel of Fig. 6R). Furthermore, we found that inhibition of miR-130-3p expression significantly increased cell viability compared with the control group after 1 and 5 h of *V. anguillarum* infection (right panel of Fig. 6R). Next, we constructed the NOD1-

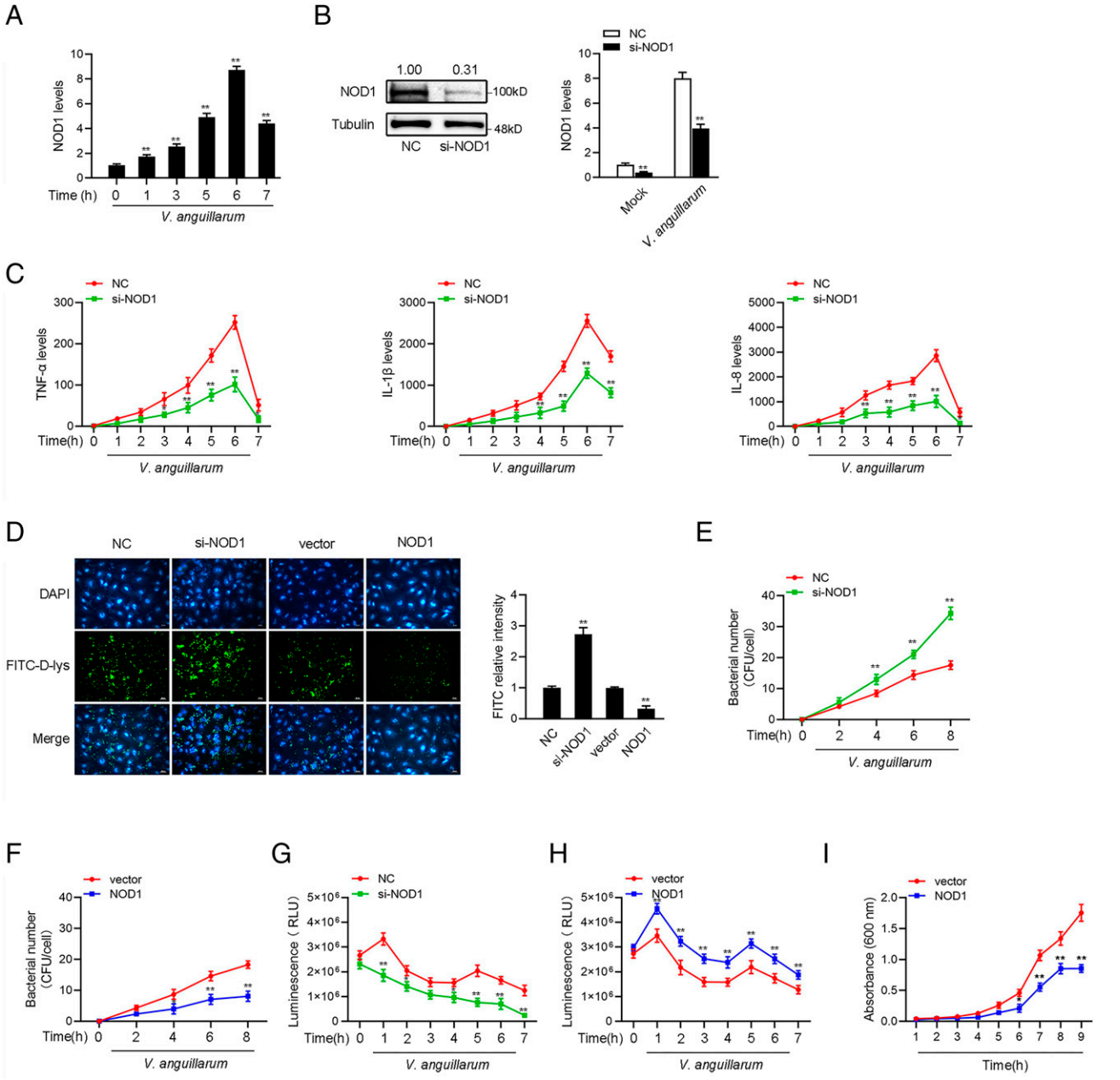

FIGURE 5. Fish NOD1 suppresses antiviral responses on *V. anguillarum* infection. (**A**) *V. anguillarum* induces an increase of NOD1 expression. The expression levels of NOD1 in MICs were measured by qPCR at the indicated time after *V. anguillarum* infection. (**B**) Knockdown of NOD1 attenuates the expression of endogenous NOD1. MICs were transfected with control siRNA (si-Ctrl) or si-NOD1 for 48 h; then the expression levels of NOD1 were determined by Western blotting and qPCR assays, respectively. (**C**) Knockdown of NOD1 attenuates the expression of inflammatory factors. MICs were transfected with si-Ctrl or si-NOD1. At 24 h posttransfection, cells were then treated with *V. anguillarum* for 24 h. The expressions of TNF-α, IL-1β, and IL-8 were determined by qPCR. (**D**) Fish NOD1 suppresses *V. anguillarum* invasion cells. MICs were transfected with si-Ctrl or NOD1-specific siRNA (si-NOD1) and pcDNA3.1 vector or NOD1 expression plasmid for 24 h, then infected with FITC-labeled *V. anguillarum* for 6 h; then it was examined by fluorescence microscope. Scale bars, 20 μm; original magnification ×400. (**E** and **F**) MKCs were transfected with si-circ or NC (E) and MICs were transfected with oe-circ or control vector (F) and then infected with *V. anguillarum.* Intracellular bacterial number was determined at different hours postinfection and shown as CFUs. (**G** and **H**) Effect of NOD1 knockdown on cell viability after *V. anguillarum* infection. MKCs were transfected with si-circ or NC (G) and MICs were transfected with oe-circ or control vector (H). At 24 h posttransfection, the cells were infected with *V. anguillarum* for different times; then cell viability assays were measured. Representative results are from three independent experiments, and statistical data are expressed as mean ± SE. (A–C) $n = 3$ biological replicates × 3 technical replicates, (D) $n = 3$ biological replicates, (E–I) $n = 3$ biological replicates × 2 technical replicates. $^{*}p < 0.05$, $^{**}p < 0.01$.

mut overexpression plasmid by cloning the mut into the pcDNA3.1 vector. In addition, a mutant type of the 3′ UTR and of the coding domain sequence region of the *M. miiuy* NOD1 gene were inserted into the pcDNA3.1 vector and detected whether miR-130-3p can influence the activity of NOD1-mut plasmid. Then the NOD1-wt or NOD1-mut, miR-130-3p, and various reporter gene plasmids were cotransfected into MKCs. The results showed that miR-130-3p could not influence the NOD1-mut on the luciferase activities of NF-κB, IL-1β, IL-8, and ISRE reporter genes (Fig. 6S). Taken together, these results suggest that NOD1 may be a direct target of miR-130-3p, which is involved in the regulation of antibacterial responses by posttranscriptional regulation of NOD1 expression.

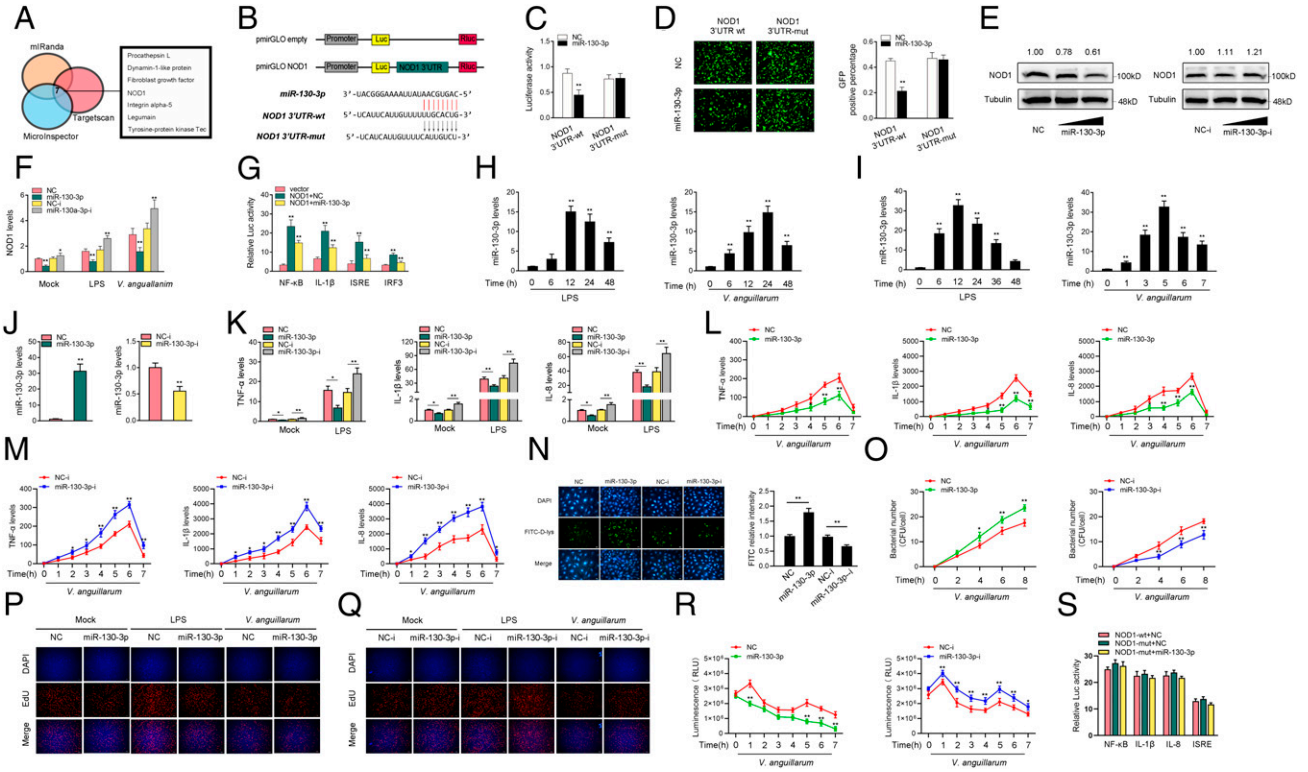

FIGURE 6. miR-130-3p suppresses antibacterial responses by targeting NOD1. (**A**) A schematic illustration showing overlapping of the targets of miR-130-3p predicted by TargetScan, miRanda, and RNAhybrid. (**B**) Schematic illustration of NOD1-wt and NOD1-mut luciferase reporter vectors. (**C**) The relative luciferase activities were detected in EPCs after cotransfection with NOD1-wt or NOD1-mut and mimics or NC. (**D**) miR-130-3p downregulated YFP expression. EPCs were cotransfected with NOD1-3′ UTR-wt or NOD1-3′ UTR-mut and mimics or NC. The fluorescence intensity and the YFP expression were evaluated by enzyme-labeled instrument. Scale bars, 20 μm; original magnification ×200. (**E** and **F**) Relative protein and mRNA levels of NOD1 were evaluated by Western blot (E) and qRT-PCR (F) in MICs after cotransfection with the miR-130-3p mimics or inhibitors. (**G**) The relative luciferase activities were detected in MICs after cotransfection with NOD1 expression plasmid, pRL-TK *Renilla* luciferase plasmid, luciferase reporter genes, NC, or mimics. (**H** and **I**) *V. anguillarum* induces an increase in miR-130-3p expression. The expression levels of miR-130-3p in intestine samples (H) and MICs (I) were measured by qPCR at an indicated time after LPS treatment or *V. anguillarum* infection. (**J**) The miR-130-3p expression levels were detected in MICs after cotransfection with NC or mimics (left panel) and NC-i or inhibitors (right panel). (**K**) qRT-PCR assays were performed to determine the expression levels of TNF-α, IL-1β, and IL-8 in cells after cotransfection with NC or mimics and cells after cotransfection with NC-i or inhibitors. (**L** and **M**) qPCR assays were performed to determine the expression levels of TNF-α, IL-1β, and IL-8 in MICs transfected with NC or mimics (L) and in MKCs transfected with NC-i or inhibitors (M) after *V. anguillarum* infection. Scale bars, 20 μm; original magnification ×400. (**N**) miR-130-3p promote *V. anguillarum* invasion cells. MKCs were transfected with NC or mimics and MICs were transfected with NC-i or inhibitors for 24 h, then infected with FITC-labeled *V. anguillarum* for 6 h, and then examined by using a fluorescence microscope. Scale bars, 20 μm; original magnification ×400. (**O**) MKCs were transfected with NC or mimics and MICs were transfected with NC-i or inhibitors and then infected with *V. anguillarum.* The intracellular bacterial number was determined at different hours postinfection and shown as CFUs. (**P** and **Q**) Cell proliferation was assessed by EdU assays in MKCs transfected with NC or mimics after LPS treated for 12 h or *V. anguillarum* infected for 6 h (P) and in MICs transfected with NC-i or inhibitors after LPS treated for 12 h or *V. anguillarum* infected for 6 h (Q). Scale bars, 20 μm; original magnification ×200. (**R**) Effect of miR-130-3p on cell viability after *V. anguillarum* infection. MKCs were transfected with NC or mimics for 24 h and MICs were transfected with NC-i or inhibitors for 24 h, then treated with *V. anguillarum* for different times. Cell viability assays were measured. (**S**) miR-130-3p could not influence the NOD1-mut on the luciferase activities of NF-κB, IL-1β, IL-8, and ISRE reporter genes. Then the NOD1-wt or NOD1-mut, miR-130-3p, and various reporter gene plasmids were cotransfected into MKCs. Representative results were from three independent experiments, and statistical data were expressed as the mean ± SE. (C) $n = 3$ biological replicates × 3 technical replicates, (D) $n = 3$ biological replicates, (E–M) $n = 3$ biological replicates × 3 technical replicates, (N) $n = 3$ biological replicates, (O) $n = 3$ biological replicates × 2 technical replicates, (P and Q) $n = 3$ biological replicates, (R and S) $n = 3$ biological replicates × 3 technical replicates. *$p < 0.05$, **$p < 0.01$.

circRNF217 acts as a sponge of miR-130-3p to enhance NOD1 expression

Given that circRNF217 could interact with miR-130-3p, miR-130-3p targets NOD1 and regulates its expression. Thus, we then tested whether circRNF217 is able to regulate NOD1. The NOD1 protein expression was significantly decreased in MKCs through knockdown of circRNF217 (Fig. 7A), although NOD1 protein expression is significantly increased when circRNF217 is overexpressed in MICs (Fig. 7B). circRNF217 expression plasmid or si-circRNF217 is transfected into MKCs, and NOD1 expression levels were detected by qRT-PCR. The results show that silencing circRNF217 would significantly reduce NOD1 expression, while circRNF217 can indeed promote NOD1 expression (Fig. 7C). To this end, we cotransfected with NOD1-3′ UTR plasmid, together with miR-130-3p, circRNF217 expression plasmid, or mutant circRNF217 expression plasmid in EPCs. Luciferase assays showed that circRNF217 could counteract the negative effect of miR-130-3p on NOD1-3′ UTR (Fig. 7D). Then the MKCs were cotransfected with miR-130-3p and circRNF217, and the Western blotting assay showed that circRNF217 could indeed reverse the inhibitory effect of miR-130-3p on NOD1 protein expression (Fig. 7E). Then the NOD1 plasmid with full-length 3′ UTR, miR-130-3p, circRNF217 plasmid, and various reporter gene plasmids was cotransfected into MKCs. The results showed that circRNF217 could reverse the negative effect of

miR-130-3p on the luciferase activities of NF-κB, IL-1β, IL-8, and ISRE reporter genes (Fig. 7F). In addition, we also confirmed that circRNF217 could significantly reduce the ability of miR-130-3p to promote the invasion of *V. anguillarum* by FITC labeling (Fig. 7G) and plate counting (Fig. 7H). Meanwhile, we attempted to explore the effect of the circRNF217/miR-130-3p regulatory loop on cell viability. The results showed that oe-circ could counteract the negative effect of miR-130-3p on cell viability on *V. anguillarum* infection (Fig. 7I). Moreover, we attempted to explore the effect of the circRNF217/miR-130-3p regulatory loop on cell proliferation. The results indicated that oe-circ could counteract the negative effect of miR-130-3p on cell proliferation on LPS or *V. anguillarum* stimulation (Fig. 7J). Collectively, these data demonstrated that circRNF217 serves as a ceRNA for miR-130-3p to regulate NOD1 expression.

circRNF217 promotes antiviral responses by targeting NOD1

To verify whether circRNF217 can play an antiviral role by targeting NOD1, we first treated MKCs with SCRV infection. During SCRV infection, the expression levels of circRNF217 were significantly increased (Fig. 8A). Then we treated MICs with SCRV infection. During SCRV infection, the expression levels of NOD1 were significantly increased (Fig. 8B). Considering that IFN-stimulating genes (ISGs) are important antiviral effectors, we focused on investigating the role of circRNF217 and NOD1 in regulating the

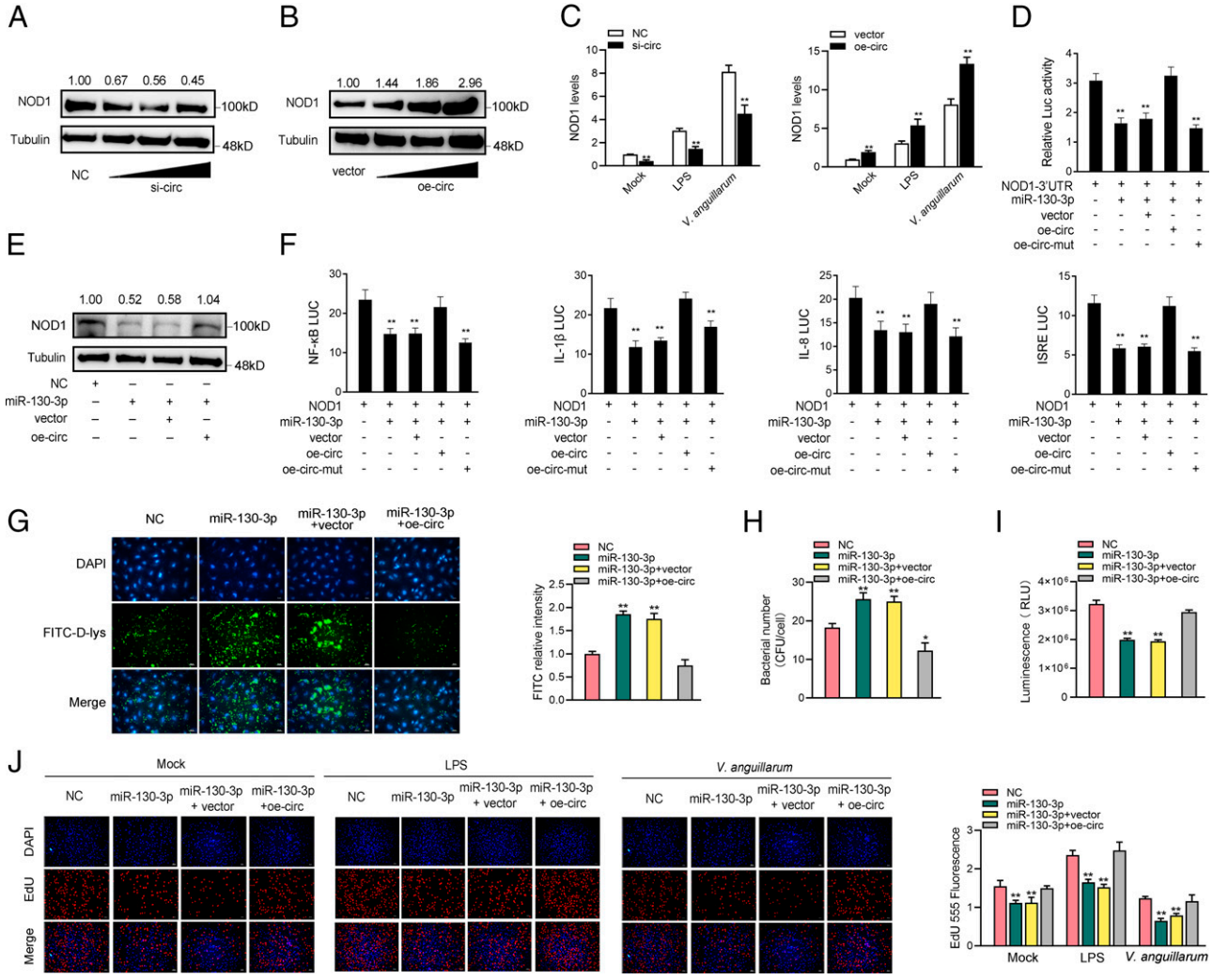

FIGURE 7. circRNF217 acts as a sponge of miR-130-3p to enhance NOD1 expression. (**A** and **B**) Relative protein levels of NOD1 in MKCs after cotransfection with si-NC or si-circ and in MICs with pcDNA3.1 vector or oe-circ expression plasmid by Western blot assays. (**C**) Relative mRNA levels of NOD1 in MKCs after cotransfection with si-NC or si-circ and in MICs with pcDNA3.1 vector or oe-circ expression plasmid by qPCR. (**D**) The relative luciferase activities were detected in EPCs after cotransfection with NOD1-3′ UTR luciferase reporter vector, NC, miR-130-3p, vector, oe-circ, or oe-circ-mut in MKCs. (**E**) Western blot assays were performed in MKCs after cotransfection with NOD1 overexpression plasmid, NC, miR-130-3p, oe-circ, or oe-circ-mut in MKCs. (**F**) oe-circ counteracts the negative effect of miR-130-3p. Relative luciferase activities were detected in MKCs after cotransfection with NOD1 expression plasmid, pRL-TK *Renilla* luciferase plasmid, luciferase reporters, NC, mimics, or oe-circ. (**G**) MKCs were cotransfected with NC, mimics, or oe-circ for 24 h, then infected with FITC-labeled *V. anguillarum* for 6 h, and then examined by fluorescence microscope. Scale bars, 20 μm; original magnification ×400. (**H**) MKCs were cotransfected with NC, mimics, or oe-circ for 24 h and then infected with *V. anguillarum*. The intracellular bacterial number was determined at different hours postinfection and shown as CFUs. (**I**) MKCs were cotransfected with NC, mimics, or oe-circ for 24 h, then treated with *V. anguillarum* for 6 h. Cell viability assays were measured. (**J**) Cell proliferation was assessed by EdU assays in MKCs after cotransfection with NC, mimics, or oe-circ. Scale bars, 20 μm; original magnification ×200. Representative results are from three independent experiments, and statistical data are expressed as the mean ± SE. (A–F) $n = 3$ biological replicates × 3 technical replicates, (G) $n = 3$ biological replicates, (H and I) $n = 3$ biological replicates × 3 technical replicates, (J) $n = 4$ biological replicates. $^{*}p < 0.05$, $^{**}p < 0.01$.

expression of ISGs and inflammatory cytokines. As shown in Fig. 8C and 8D, the oe-circ (Fig. 8C) and NOD1 (Fig. 8D) also could significantly inhibit the expression levels of inflammatory cytokines (TNF-α) and antiviral genes such as myxovirus resistance protein 1 and ISG15 after SCRV infection. By contrast, knockdown of circRNF217 (Fig. 8C) and NOD1 (Fig. 8D) also increased the expression levels of these genes under SCRV treatment. In addition, we found that circRNF217 could counteract the promoting effect of miR-130-3p on SCRV replication (Fig. 8E), and the result showed that oe-circ could counteract the negative effect of miR-130-3p on cell viability on SCRV infection (Fig. 8F). By measuring the SCRV median tissue culture-infective dose levels in the supernatant from the infected MKCs, we found that knockdown of circRNF217 significantly inhibited SCRV replication after 48 and 72 h of SCRV infection (Fig. 8G).

The ceRNA network of regulating NOD1 is widely found in teleost fish

To address the generality of our findings, we tested whether this regulatory network exists in other fish. As shown in Fig. 9A, we first tested whether miR-130-3p can target the NOD1 3′ UTR. Luciferase reporter plasmids were generated by cloning the NOD1-3′ UTR of *S. ocellatus* and *N. diacanthus* into the pmirGLO vector, within the mutant devoid of a miR-130-3p binding site as a control. Strikingly, miR-130-3p mimics were sufficient to decrease luciferase activities when respectively cotransfected with the wild-types of *S. ocellatus* and *N. diacanthus* NOD1-3′ UTR, whereas they show no effect on the luciferase activity of cells transfected with their mutant types (Fig. 9B). These results indicate that miR-130-3p can target the NOD1 gene in other fish species. In addition, we also verified the findings that miR-130-3p regulating circRNF217 also exists in other species. To this end, we first examined the sequence alignment of circRNF217 among different species. Interestingly, the sequence of circRNF217 is highly conserved among different fish species. Particularly, circRNF217 in these different species presents highly conserved in the binding sites of miR-130-3p (Fig. 9C). Then, we produced luciferase constructs of *S. ocellatus* and *N. diacanthus* and thus circRNF217 and their mutated forms with miR-130-3p binding sites mutated to investigate whether circRNF217 in other fish species could also interact with miR-130-3p. Luciferase assays revealed that miR-130-3p can suppress the luciferase activity of the wild-type of circRNF217 luciferase plasmid in both species, but it has no effect on mutated forms (Fig. 9D). Furthermore, to test whether *S. ocellatus* and *N. diacanthus* circRNF217 can affect miR-130-3p activity, we conducted luciferase assays and found that both *S. ocellatus* and *N. diacanthus* circRNF217 could counteract the inhibitory effect of miR-130-3p on NOD1 (Fig. 9E, 9F). These results indicate that circRNF217 may act as endogenous sponge RNA to interact with miR-130-3p among different fish. All of these data suggest that circRNF217 contains relatively conserved elements among different fish species, which is very important for preserving their functions (Fig. 9G).

Discussion

According to reports, NOD1 can be used as an immune-related intracellular receptor, playing an important role in sensing and resisting the invasion of pathogens, such as viruses or bacteria (40, 41). It can detect different pathogenic components of Gram-negative bacteria and activate related signal transduction processes to promote inflammation (42). Recent studies have confirmed that in bony fish, NOD1 can be used as a receptor for the bacterial pathogenic component LPS and can also be used as a receptor for RNA viruses to activate the immune response process. For example, miiuy croaker NOD1 can recognize LPS and γ-D-glutamyl-meso-diaminopimelic acid, thereby activating the NF-κB signaling pathway, promoting the production of inflammatory factors, and resisting bacterial invasion (5, 6). NOD1 can recognize and bind to SVCV (ssRNA virus), induce the production of IFN and ISGs, and enhance the antiviral immune response (9). Moreover, in our previous studies, we have verified that the SCRV (dsRNA virus) can induce NOD1-dependent signaling pathways (43). Of course, the innate immune response initiated by the NOD1 receptor often requires the participation of a series of regulatory factors, including some coding genes and noncoding genes. In this study, we found that two noncoding genes,

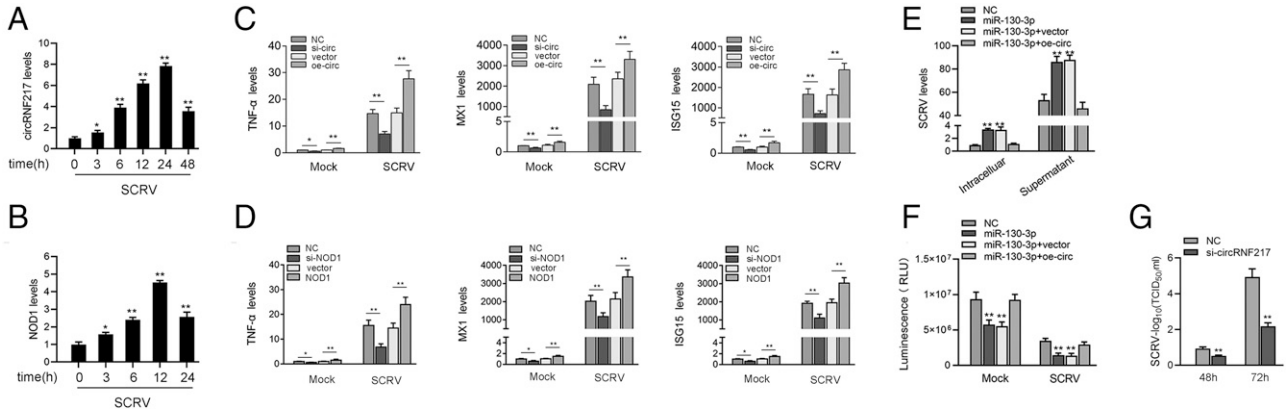

FIGURE 8. circRNF217 suppresses antiviral responses by targeting NOD1. (**A**) The expression levels of circRNF217 in MKCs were measured by qRT-PCR at the indicated time after SCRV infection. (**B**) The expression levels of NOD1 in MICs were measured by qRT-PCR at the indicated time after SCRV infection. (**C**) qPCR assays were performed to determine the expression levels of TNF-α, IL-1β, and IL-8 in MICs transfected with overexpression plasmid (oe-circ) or control vector (pLC5-ciR) and in MKCs transfected with (si-circRNF217-1) si-circ or NC after SCRV treatment. (**D**) qPCR assays were performed to determine the expression levels of TNF-α, IL-1β, and IL-8 in MICs transfected with NOD1 overexpression plasmid or control vector and in MKCs transfected with si-NOD1 or NC after SCRV treatment. (**E**) SCRV RNA expression was assessed by qPCR in MICs after cotransfection with NC, mimics, or oe-circ. (**F**) Cell viability was assessed by ATP viability assays in MICs after cotransfection with NC, mimics, or oe-circ. (**G**) MKCs were transfected with NC or si-circRNF217 and infected with SCRV at MOI 5 for 1 h, washed, and then added with fresh medium. After 48 and 72 h, SCRV tissue culture-infective dose in cultural supernatants was measured with MKCs. Representative results are from three independent experiments, and statistical data are expressed as mean ± SE. (A and B) $n = 3$ biological replicates × 3 technical replicates, (C–G) $n = 3$ biological replicates × 2 technical replicates. $^{*}p < 0.05$, $^{**}p < 0.01$.

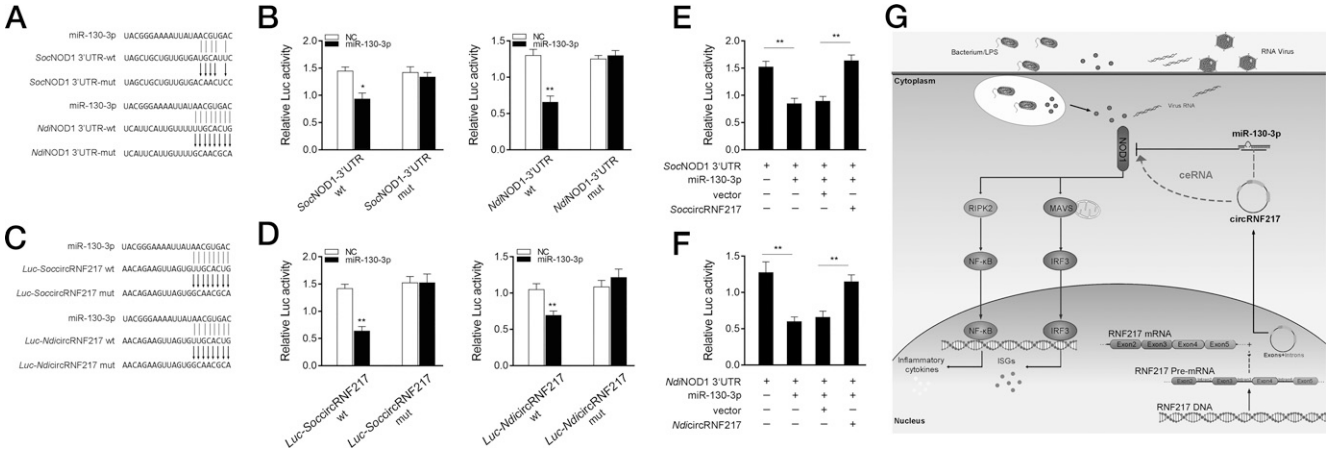

FIGURE 9. The ceRNA network of regulating NOD1 is widely found in teleost fish. (**A**) A putative miR-130-3p-binding site of NOD1-3′ UTR in *Soc* (up) and *Ndi* (down). (**B**) The relative luciferase activities were detected in EPCs after cotransfection with *Soc*-NOD1-wt or *Soc*-NOD1-mut and miR-130-3p or NC (left) and cells after cotransfection with *Ndi*-NOD1L-wt or *Ndi*-NOD1-mut and miR-130-3p or NC (right). (**C**) A putative miR-130-3p binding site of Luc-*Soc*-circRNF217 (up) and Luc-*Ndi*-circRNF217 (down). (**D**) The relative luciferase activities were detected in EPCs after cotransfection with *Soc*-circRNF217-wt or *Soc*-circRNF217-mut and miR-130-3p or NC (left) and in cells after cotransfection with Ndi-circRNF217-wt or Ndi-circRNF217-mut and miR-130-3p or NC (right). (**E** and **F**) The relative luciferase activities were detected in EPCs after cotransfection with *Soc*-NOD1-3′ UTR luciferase reporter vector, NC, miR-130-3p, or *Soc*-circRNF217 (E) and in EPCs after cotransfection with *Ndi*-NOD1-3′ UTR luciferase reporter vector, NC, miR-130-3p, or *Ndi*-circRNF217 (F). (**G**) Schematic diagram of the mechanism underlying circRNF217 as a ceRNA for miR-130-3p to regulate NOD1 expression. NOD1 recognizes the PAMPs of bacteria in the cytoplasm. After activation, NOD1 recruits RIPK2 and activates NF-κB, which eventually leads to NF-κB entry into the nucleus and activates the transcription of inflammatory factors. In addition, NOD1 can also be activated by single-stranded or double-stranded viral RNA and further promote the activation of MAVS, leading to the activation and nuclear entry of IRF3, and finally leading to the transcription of antiviral genes, such as ISGs. miR-130-3p targets NOD1 and represses NOD1-mediated innate responses, thereby regulating bacterial invasion and virus replication. circRNF217 acts as a molecular sponge regulating miR-130-3p to enhance NOD1 expression, thereby maintaining the stable antibacterial and antiviral responses. Representative results are from three independent experiments, and statistical data are expressed as the mean ± SE. (B) $n = 3$ biological replicates × 3 technical replicates, and (D–F) $n = 3$ biological replicates × 3 technical replicates. $^*p < 0.05$, $^{**}p < 0.01$.

miR-130-3p and circRNF217, negatively regulate and positively regulate NOD1, respectively, and maintain the body's immune balance.

As a kind of important regulatory factor, ncRNA has been widely studied. A large number of studies have shown that ncRNA can participate in a variety of cell biological processes, such as proliferation, differentiation, development, and cell proliferation (44–49). At present, ncRNA has been studied extensively in mammals, and the research system has been very successful, but there is not much research in lower vertebrates. However, in recent decades, ncRNA research in lower vertebrates, especially in bony fish, has also made some progress. For example, miiuy croaker small ncRNA miR-3570 can inhibit the expression of MyD88 and MAVS, thereby regulating excessive inflammation and inherent antiviral response (50–52). Moreover, it has been reported that the regulatory mechanisms of long ncRNA NARL, IRL, MARL, and AANCR all can regulate the innate immune response of miiuy croaker through the ceRNA mechanism (43, 51–55). In addition to the small ncRNA and long ncRNA mentioned earlier, there is a new type of ncRNA that has attracted great attention, namely, circRNA. Current studies have shown that the majority of circRNA originates from protein coding host genes. Therefore, it is very necessary to study the relationship between circRNA and its host gene, because there may be a strong connection between them, or the expression of circRNA may be independently regulated and has no strong correlation with its host gene. The relationship between circRNA and its host gene can be classified according to the expression of circRNA relative to its host gene. For example, the expression level of circRNA may be coupled with the expression level of the host gene; that is, if the expression of the host gene increases, the expression of circRNA will follow this trend. Of course, the opposite may also occur, so studying the relationship between circRNA and its host gene is undoubtedly a very important premise for the study of circRNA function. A large number of studies show that circRNA has the same function as lncRNA and can form a ceRNA regulatory network with miRNA. It regulates mRNA expression through competition and sharing miRNA (miRNA response element) and regulates gene expression after transcriptional regulation (56). In addition, circRNA has another feature that has attracted great attention. circRNA has high stability in vitro because of its special shear formation mode, and its plate decay period in vitro is much longer than most ncRNAs, which means that these circRNAs with important regulatory effects will have great potential to be developed into drugs with excellent regulatory effects (56, 57). Current studies show that a large number of EcircRNAs have been found to function through the ceRNA mechanism (57), and only a few studies show that EIcircRNAs can also function through the ceRNA mechanism. At present, a large number of circRNAs mainly focus on cancer and antiviral effects (58). It is still very unclear whether circRNAs have antibacterial functions. Among lower vertebrates, especially teleost fish, the greatest risk often comes from bacteria, especially those with high mortality and widespread distribution. The most typical is *V. anguillarum*. The economic losses of the aquatic industry caused by *V. anguillarum* every year are very large. Therefore, it is urgent to deeply study the infection mechanism related to *V. anguillarum*. In this study, we identified a new EIcircRNA, called circRNF217, which could promote antibacterial immune response caused by *V. anguillarum* through a ceRNA mechanism in miiuy croaker. We found that EIcircRNA-circRNF217 can be located in the cytoplasm, which is the basis for its biological function. Also, the results showed that circRNF217 was significantly upregulated by treatment with *V. anguillarum* or LPS at different time points, but not *RNF217*. Therefore, we speculate that the increase of circRNF217 expression after *V. anguillarum* or LPS stimulation may not be caused by the change of *RNF217* expression. Moreover, we

identified a new small ncRNA called miR-130-3p in miiuy croaker. miR-130-3p could negatively regulate the expression of NOD1 and inhibit the production of inflammatory factors mediated by NOD1, thereby avoiding excessive inflammation and promoting bacterial invasion into cells. This negative regulatory mechanism may be beneficial to the host's self-protection after bacterial infection to escape the host's antibacterial immune response and survive. However, circRNF217 promoted the antibacterial effect of NOD1 and weakened the infection of *V. anguillarum* by competitively adsorbing miR-130-3p. The earlier results indicate that circRNF217 can be used as a new immunomodulatory molecule to participate in the regulation of teleost antibacterial response.

Because the study reported that NOD1 not only has the function of recognizing LPS but also recognizes viral RNA, we further verified whether circRNF217 can also enhance the antiviral immune response by competitive inhibition of miR-130-3p. The results were very exciting; we found that the expression of circRNF217 increased significantly under the stimulation of SCRV virus, and the results showed that miR-130-3p could promote the replication of SCRV virus, while circRNF217 could inhibit the replication of virus by inhibiting miR-130-3p, thereby enhancing the antiviral immune response. Therefore, circRNA is a very important regulatory factor, which can regulate not only the antibacterial immune response but also the antiviral immune response. As such an important target molecule, circRNA is of great significance in the process of disease resistance in lower vertebrates.

In this study, we discovered a new EIcircRNA, circRNF217, which plays an active role in the inflammation and antibacterial response of teleost fish. We found that miR-130-3p played a negative role in inflammation and antibacterial response, and promote bacterial invasion of cells in miiuy croaker. On the contrary, circRNF217 played a positive role in NOD1-mediated antibacterial responses. We confirmed that the mechanism of the two ncRNAs played a role in regulating the innate antibacterial immune responses. circRNF217 could be used as the ceRNA of miR-130-3p to reduce its inhibitory effect on NOD1 expression, thereby inhibiting the bacterial invasion of cells. In addition, we also found that circRNF217 can also weaken the inhibitory effect of miR-130-3p on NOD1 through a ceRNA mechanism, so as to promote NOD1 to inhibit the replication of SCRV virus and enhance the antiviral immune response. In addition, we also found that the structure and function of circRNF217 were highly conserved in different teleost fish. In summary, our results not only elucidate the biological mechanism of the circRNA–miRNA–mRNA axis in antibacterial immune responses of fish but also provide new insights for understanding the impact of circRNA on host–pathogen interactions and formulating fish disease prevention of resistance.

Disclosures

The authors have no financial conflicts of interest.

References

1. Hatinguais, R., J. A. Willment, and G. D. Brown. 2020. PAMPs of the fungal cell wall and mammalian PRRs. *Curr. Top. Microbiol. Immunol.* 425: 187–223.
2. Zhou, Y., C. He, L. Wang, and B. Ge. 2017. Post-translational regulation of antiviral innate signaling. *Eur. J. Immunol.* 47: 1414–1426.
3. Mogensen, T. H. 2009. Pathogen recognition and inflammatory signaling in innate immune defenses. *Clin. Microbiol. Rev.* 22: 240–273.
4. Kim, Y. K., J.-S. Shin, and M. H. Nahm. 2016. NOD-like receptors in infection, immunity, and diseases. *Yonsei Med. J.* 57: 5–14.
5. Chamaillard, M., M. Hashimoto, Y. Horie, J. Masumoto, S. Qiu, L. Saab, Y. Ogura, A. Kawasaki, K. Fukase, S. Kusumoto, et al. 2003. An essential role for NOD1 in host recognition of bacterial peptidoglycan containing diaminopimelic acid. *Nat. Immunol.* 4: 702–707.
6. Roy, A. C., G. Chang, N. Ma, Y. Wang, S. Roy, J. Liu, Z. U. Aabdin, and X. Shen. 2019. Sodium butyrate suppresses NOD1-mediated inflammatory molecules expressed in bovine hepatocytes during iE-DAP and LPS treatment. *J. Cell. Physiol.* 234: 19602–19620.
7. Zhang, J., X. Kong, C. Zhou, L. Li, G. Nie, and X. Li. 2014. Toll-like receptor recognition of bacteria in fish: ligand specificity and signal pathways. *Fish Shellfish Immunol.* 41: 380–388.
8. Bi, D., Y. Wang, Y. Gao, X. Li, Q. Chu, J. Cui, and T. Xu. 2018. Recognition of lipopolysaccharide and activation of NF-κB by cytosolic sensor NOD1 in teleost fish. *Front. Immunol.* 9: 1413.
9. Wu, X. M., J. Zhang, P. W. Li, Y. W. Hu, L. Cao, S. Ouyang, Y. H. Bi, P. Nie, and M. X. Chang. 2020. NOD1 promotes antiviral signaling by binding viral RNA and regulating the interaction of MDA5 and MAVS. *J. Immunol.* 204: 2216–2231.
10. Yamamoto-Furusho, J. K., N. Barnich, R. Xavier, T. Hisamatsu, and D. K. Podolsky. 2006. Centaurin β1 down-regulates nucleotide-binding oligomerization domains 1- and 2-dependent NF-kappaB activation. *J. Biol. Chem.* 281: 36060–36070.
11. Hahn, J.-S. 2005. Regulation of Nod1 by Hsp90 chaperone complex. *FEBS Lett.* 579: 4513–4519.
12. da Silva Correia, J., Y. Miranda, N. Leonard, and R. Ulevitch. 2007. SGT1 is essential for Nod1 activation. *Proc. Natl. Acad. Sci. USA* 104: 6764–6769.
13. Sanger, H. L., G. Klotz, D. Riesner, H. J. Gross, and A. K. Kleinschmidt. 1976. Viroids are single-stranded covalently closed circular RNA molecules existing as highly base-paired rod-like structures. *Proc. Natl. Acad. Sci. USA* 73: 3852–3856.
14. Hansen, T. B., T. I. Jensen, B. H. Clausen, J. B. Bramsen, B. Finsen, C. K. Damgaard, and J. Kjems. 2013. Natural RNA circles function as efficient microRNA sponges. *Nature* 495: 384–388.
15. Cocquerelle, C., B. Mascrez, D. Hétuin, and B. Bailleul. 1993. Mis-splicing yields circular RNA molecules. *FASEB J.* 7: 155–160.
16. Jeck, W. R., J. A. Sorrentino, K. Wang, M. K. Slevin, C. E. Burd, J. Liu, W. F. Marzluff, and N. E. Sharpless. 2013. Circular RNAs are abundant, conserved, and associated with ALU repeats. *RNA* 19: 141–157.
17. Liu, J., T. Liu, X. Wang, and A. He. 2017. Circles reshaping the RNA world: from waste to treasure. *Mol. Cancer* 16: 58.
18. Panda, A. C. 2018. Circular RNAs act as miRNA sponges. *Adv. Exp. Med. Biol.* 1087: 67–79.
19. Rong, D., H. Sun, Z. Li, S. Liu, C. Dong, K. Fu, W. Tang, and H. Cao. 2017. An emerging function of circRNA-miRNAs-mRNA axis in human diseases. *Oncotarget* 8: 73271–73281.
20. Huang, A., H. Zheng, Z. Wu, M. Chen, and Y. Huang. 2020. Circular RNA-protein interactions: functions, mechanisms, and identification. *Theranostics* 10: 3503–3517.
21. Zhang, M., N. Huang, X. Yang, J. Luo, S. Yan, F. Xiao, W. Chen, X. Gao, K. Zhao, H. Zhou, et al. 2018. A novel protein encoded by the circular form of the SHPRH gene suppresses glioma tumorigenesis. *Oncogene* 37: 1805–1814.
22. Lu, T. X., and M. E. Rothenberg. 2018. MicroRNA. *J. Allergy Clin. Immunol.* 141: 1202–1207.
23. Wang, X., H. Jin, S. Jiang, and Y. Xu. 2018. MicroRNA-495 inhibits the high glucose-induced inflammation, differentiation and extracellular matrix accumulation of cardiac fibroblasts through downregulation of NOD1. *Cell. Mol. Biol. Lett.* 23: 23.
24. Kang, H., Y. Park, A. Lee, H. Seo, M. J. Kim, J. Choi, H. N. Jo, H. N. Jeong, J. G. Cho, W. Chang, et al. 2017. Negative regulation of NOD1 mediated angiogenesis by PPARγ-regulated miR-125a. *Biochem. Biophys. Res. Commun.* 482: 28–34.
25. Magnadóttir, B. 2006. Innate immunity of fish (overview). *Fish Shellfish Immunol.* 20: 137–151.
26. Su, H., R. Chang, W. Zheng, Y. Sun, and T. Xu. 2021. microRNA-210 and microRNA-3570 negatively regulate NF-κB-mediated inflammatory responses by targeting RIPK2 in teleost fish. *Front. Immunol.* 12: 961.
27. Luis, A. I. S., E. V. R. Campos, J. L. de Oliveira, M. Guilger-Casagrande, R. de Lima, R. F. Castanha, V. L. S. S. de Castro, and L. F. Fraceto. 2020. Zein nanoparticles impregnated with eugenol and garlic essential oils for treating fish pathogens. *ACS Omega* 5: 15557–15566.
28. Gon Choudhury, T., V. Tharabenahalli Nagaraju, S. Gita, A. Paria, and J. Parhi. 2017. Advances in bacteriophage research for bacterial disease control in aquaculture. *Rev. Fish. Sci. Aquac.* 25: 113–125.
29. Defoirdt, T. 2014. Virulence mechanisms of bacterial aquaculture pathogens and antivirulence therapy for aquaculture. *Rev. Fish. Sci. Aquac.* 6: 100–114.
30. Frans, I., C. W. Michiels, P. Bossier, K. A. Willems, B. Lievens, and H. Rediers. 2011. *Vibrio* anguillarum as a fish pathogen: virulence factors, diagnosis and prevention. *J. Fish Dis.* 34: 643–661.
31. Hickey, M. E., and J. L. Lee. 2018. A comprehensive review of *Vibrio* (Listonella) anguillarum: ecology, pathology and prevention. *Rev. Aquac.* 10: 585–610.
32. Cui, J., Q. Chu, and T. Xu. 2016. miR-122 involved in the regulation of toll-like receptor signaling pathway after *Vibrio* anguillarum infection by targeting TLR14 in miiuy croaker. *Fish Shellfish Immunol.* 58: 67–72.
33. Trapnell, C., A. Roberts, L. Goff, G. Pertea, D. Kim, D. R. Kelley, H. Pimentel, S. L. Salzberg, J. L. Rinn, and L. Pachter. 2012. Differential gene and transcript expression analysis of RNA-seq experiments with TopHat and Cufflinks. [Published erratum appears in 2014 *Nat. Protoc.* 9: 2513.] *Nat. Protoc.* 7: 562–578.
34. Kim, D., and S. L. Salzberg. 2011. TopHat-Fusion: an algorithm for discovery of novel fusion transcripts. *Genome Biol.* 12: R72.
35. Gao, Y., J. Wang, Y. Zheng, J. Zhang, S. Chen, and F. Zhao. 2016. Comprehensive identification of internal structure and alternative splicing events in circular RNAs. *Nat. Commun.* 7: 12060.

36. Fu, X., Q. Lin, H. Liang, L. Liu, Z. Huang, N. Li, and J. Su. 2017. The biological features and genetic diversity of novel fish rhabdovirus isolates in China. *Arch. Virol.* 162: 2829–2834.
37. Livak, K. J., and T. D. Schmittgen. 2001. Analysis of relative gene expression data using real-time quantitative PCR and the 2(-Δ Δ C(T)) Method. *Methods* 25: 402–408.
38. John, B., A. J. Enright, A. Aravin, T. Tuschl, C. Sander, and D. S. Marks. 2004. Human MicroRNA targets. [Published erratum appears in 2005 *PLoS Biol.* 3: e264.] *PLoS Biol.* 2: e363.
39. Rusinov, V., V. Baev, I. N. Minkov, and M. Tabler. 2005. MicroInspector: a web tool for detection of miRNA binding sites in an RNA sequence. *Nucleic Acids Res.* 33(Web Server): W696–W700.
40. Li, F., and J. Xiang. 2013. Signaling pathways regulating innate immune responses in shrimp. *Fish Shellfish Immunol.* 34: 973–980.
41. Shin, W. G., B. J. Park, S. J. Lee, and J. G. Kim. 2018. Infection of human intestinal epithelial cells by invasive bacteria activates NF-κB and increases ICAM-1 expression through NOD1. *Korean J. Intern. Med. (Korean. Assoc. Intern. Med.)* 33: 81–90.
42. Vegna, S., D. Gregoire, M. Moreau, P. Lassus, D. Durantel, E. Assenat, U. Hibner, and Y. Simonin. 2016. NOD1 participates in the innate immune response triggered by hepatitis C virus polymerase. *J. Virol.* 90: 6022–6035.
43. Zheng, W., Q. Chu, and T. Xu. 2021. The long noncoding RNA NARL regulates immune responses via microRNA-mediated NOD1 downregulation in teleost fish. *J. Biol. Chem.* 296: 100414.
44. Wang, M., F. Yu, W. Wu, Y. Zhang, W. Chang, M. Ponnusamy, K. Wang, and P. Li. 2017. Circular RNAs: a novel type of non-coding RNA and their potential implications in antiviral immunity. *Int. J. Biol. Sci.* 13: 1497–1506.
45. Sharma, N., and S. K. Singh. 2016. Implications of non-coding RNAs in viral infections. *Rev. Med. Virol.* 26: 356–368.
46. Wang, H., Z. Tan, H. Hu, H. Liu, T. Wu, C. Zheng, X. Wang, Z. Luo, J. Wang, S. Liu, et al. 2019. microRNA-21 promotes breast cancer proliferation and metastasis by targeting LZTFL1. *BMC Cancer* 19: 738.
47. Wu, R., J. Zeng, J. Yuan, X. Deng, Y. Huang, L. Chen, P. Zhang, H. Feng, Z. Liu, Z. Wang, et al. 2018. MicroRNA-210 overexpression promotes psoriasis-like inflammation by inducing Th1 and Th17 cell differentiation. *J. Clin. Invest.* 128: 2551–2568.
48. Zhao, X. Q., Y. Ao, H. Y. Chen, and H. Wang. 2020. [The role of miRNA in kidney development]. *Yi Chuan* 42: 1062–1072.
49. Essandoh, K., Y. Li, J. Huo, and G.-C. Fan. 2016. MiRNA-mediated macrophage polarization and its potential role in the regulation of inflammatory response. *Shock* 46: 122–131.
50. Chu, Q., Y. Sun, J. Cui, and T. Xu. 2017. MicroRNA-3570 modulates the NF-κB pathway in teleost fish by targeting MyD88. *J. Immunol.* 198: 3274–3282.
51. Xu, T., Q. Chu, J. Cui, and D. Bi. 2018. Inducible MicroRNA-3570 feedback inhibits the RIG-I-dependent innate immune response to Rhabdovirus in teleost fish by targeting MAVS/IPS-1. J. Virol. 92: e01594-17.
52. Zheng, W., Q. Chu, and T. Xu. 2021. Long noncoding RNA IRL regulates NF-κB-mediated immune responses through suppression of miR-27c-3p-dependent IRAK4 downregulation in teleost fish. *J. Biol. Chem.* 296: 100304.
53. Chu, Q., T. Xu, W. Zheng, R. Chang, and L. Zhang. 2020. Long noncoding RNA MARL regulates antiviral responses through suppression miR-122-dependent MAVS downregulation in lower vertebrates. *PLoS Pathog.* 16: e1008670.
54. Chu, Q., T. Xu, W. Zheng, R. Chang, and L. Zhang. 2021. Long noncoding RNA AANCR modulates innate antiviral responses by blocking miR-210-dependent MITA downregulation in teleost fish, Miichthys miiuy. *Sci. China Life Sci.* 64: 1131–1148.
55. An, Y., K. L. Furber, and S. Ji. 2017. Pseudogenes regulate parental gene expression via ceRNA network. *J. Cell. Mol. Med.* 21: 185–192.
56. Han, J. Y., S. Guo, N. Wei, R. Xue, W. Li, G. Dong, J. Li, X. Tian, C. Chen, S. Qiu, et al. 2020. ciRS-7 promotes the proliferation and migration of papillary thyroid cancer by negatively regulating the miR-7/epidermal growth factor receptor axis. *BioMed Res. Int.* 2020: 9875636.
57. Wang, Y., J. Li, C. Du, L. Zhang, Y. Zhang, J. Zhang, and L. Wang. 2019. Upregulated circular RNA circ-UBE2D2 predicts poor prognosis and promotes breast cancer progression by sponging miR-1236 and miR-1287. *Transl. Oncol.* 12: 1305–1313.
58. Zhang, X., P. Luo, W. Jing, H. Zhou, C. Liang, and J. Tu. 2018. circSMAD2 inhibits the epithelial-mesenchymal transition by targeting miR-629 in hepatocellular carcinoma. *OncoTargets Ther.* 11: 2853–2863.